LAPPEENRANTA-LAHTI UNIVERSITY OF TECHNOLOGY LUT
LUT School of Energy Systems
Electrical Engineering

Shahab Khalghani

ANALYTICAL LOSS CALCULATION TOOL FOR AN INDUCTION MOTOR

Examiners: Professor Juha Pyrhönen
Dr. Lassi Aarniovuori

ABSTRACT

Lappeenranta-Lahti University of Technology LUT
LUT School of Energy Systems
Degree Programme in Electrical Engineering

Shahab Khalghani

Analytical loss calculation tool for an induction motor

Master's thesis
Year of completion of the thesis 2020
33 pages, 13 figures, 7 tables and 3 appendices
Examiners: Professor J. Pyrhönen and Dr. L. Aarniovuori

Keywords:
Induction Motor, Iron Losses, Copper Losses, Mechanical Losses, Additional Losses, Efficiency

This thesis introduces an analytical loss calculation tool which is able to predicate the loss components and efficiency of a specific 5 kW induction motor powered by a converter. The calculation tool functions in different operation modes in where voltage, frequency, torque and temperature are variables. The way the tool constitutes is illustrated with equations and relative descriptions. At the end of this thesis, analytical results gained by the already mentioned tool were weighted with real measured results given by LUT laboratory. The comparison proves the competence of this decent tool for estimating the loss components, predicating the efficiency and other extra information such as maximum torque, power factor, and impedance in rotor and stator.

ACKNOWLEDGEMENTS

First and foremost, I would like to deeply appreciate my examiners Professor Juha Pyrhönen, Dr. Lassi Aarniovuori and Dr. Pia Lindh for their encouragement and their continuous support to my Master's thesis. Their patience, immense knowledge and fast responses to my emails were quite sincerely practical. Their aid smoothed my way with less barriers to gain the achievement we were expecting to acquire.

Next, I would thank to Dr. Katja Hynynen for her warm contribution and advices in the beginning of my Master's program and also other hardworking professors and teachers in LUT University in electrical department for their affairs and enthusiasm.

Last but not the least, I express my pure gratitude to my parent and my elder brother for the heartfelt financial support and genuine motivation.

Finally, my thanks to all individuals including my classmates, teammates, friends etc. who have aided me to complete my Master's program directly or indirectly.

Date 02.12.2020
Shahab Khalghani

TABLE OF CONTENTS

ABBREVIATIONS AND SYMBOLS

Acronyms

CFD	Computational Fluid Dynamic
DC	Direct Current
EPRI	Electric Power Research Institute
IEC	International Electrotechnical Commission
IM	Induction Motor
RMS	Root Mean Square
TS	Technical Specification

Roman variables

a	number of parallel branches
A	linear regression constant (slope)
b	tooth width
B	linear regression constant (value at zero)
D	diameter
E	air gap induced voltage
f	frequency
h	height
I	current RMS value
k	correction factor
l	core length
m	number of phases
n	rotational speed
N	number of coil turns
p	number of pole pairs
P	power or losses
Q	number of rotor or stator slots
R	resistance
s	slip
S	cross sectional area
T	torque or temperature

U	voltage or magnetic voltage
v	velocity
V	volume
X	inductance
Z	impedance

Greek variables

α	temperature coefficient
δ	air gap
η	efficiency
μ	permeability
ρ	referring factor or density
σ	conductivity
τ	pole or slot pitch
ω	angular speed

Subscripts

0	initial or reference
av	average
al	aluminium
bar	rotor bar
c	copper
cr	copper loss in rotor
cs	copper loss in stator
e	electric or eddy current
E	electric
eddy	eddy current loss
ef	effective
fw	friction and windage
Fe	iron, core
Fe,ys	iron in stator yoke
Fe,ds	iron in stator tooth
h	hysteresis
hyst	hysteresis
in	input

LL	linear (voltage)
m	maximum or air gap or magnetizing
mdr	magnetic rotor tooth
mds	magnetic stator tooth
mech	mechanic
myr	magnetic rotor yoke
mys	magnetic stator yoke
mδe	magnetic equivalent air gap
n	nominal
out	output
p	pole, pole pitch or related to bearing and windage
phase	voltage phase
r	rotor
ring	rotor ring
s	stator
sq	skewing
st	stray losses
te	temprature depended of eddy current
th	temprature depended of hysteresis
total	total losses
ur	rotor slot
us	stator slot
v	subscribt of multiplying factor
w	winding
w1	fundamental winding
ys	stator yoke
σ	related to leakage inductance

1 INTRODUCTION

The consumption of electric motors was estimated to be 30-80% of the industrial global electricity generated. Most of these motors are induction motors (IMs). Specifically, within European continent, the share of IMs is counted as 65-72% (Hasanuzzaman, 2010). Induction motor and especially squirrel-cage motor are widespreadly utilized in electrical drives. Therefore, even a small fraction of efficiency improvement in induction motors can drastically reduce the worldwide electricity consumption.

Electric power research institute (EPRI) provided a report saying that 60-65% of industrial motors are working at lower than 60% of their nominal load capacity. The remaining 35-40% of motors are eternally dissipating the electricity because of poor efficiency caused to partial loading (Choudhary et al, 2015).

There are, in general, three ways to reduce these dissipations namely, 1. applying an appropriate control procedure; 2. betterment of waveforms generated by inverters; and 3. motor selection and design (Cao-Minh Ta and Hori, 2001). In this Master's thesis, the losses on number 3 are examined for a specific 5 kW induction motor. The most significant losses in the motor, namely, iron losses, copper losses, mechanical and stray losses, were analytically examined at a spread range of operational points.

The target is to establish a tool for calculating and analyzing the losses and efficiency of a specific squirrel cage induction motor. The model is applicable at different excitation frequencies and load values. Once analytical values of losses were acquired, they were weighted with the real measured result gathered by LUT university laboratory. In the last sections of this Master's thesis, the accuracy of this tool will be demonstrated.

Before probing the tool, a general introduction to diverse losses happening in an electrical motor is required. There are two major types of losses. These losses are categorized as (Hasanuzzaman, 2010),

- Variable losses.
- Constant or fixed losses

Constant or fixed losses are introduced as losses that are assumed to remain constant upon the regular operating modes of induction motor. Through executing a no load test on induction motor, the amplitudes of constant losses are comfortably earned. Well-known examples of the fixed losses are (Hasanuzzaman, 2010),

- Mechanical losses
- Iron or core losses,

Eddy current and hysteresis losses are belonged to iron losses. To diminish eddy current losses, utilization of lamination on core is suggested. Suitable steel lamination makes the areas of core smaller and meanwhile; the resistance enhances that consequently makes eddy current loss minimized. Regarding hysteresis loss, application of a high-grade silicon steel, is a solution for elimination of this loss. Frequency of supply voltage that is equivalent with stator frequency can extremely influence core losses. If stator frequency is multiplied by per-unit rotor slip, rotor frequency is achieved that obviously this rotor frequency would be a minor fraction of stator frequency. For example, in this specific 5 kW motor at stator frequency of 50 Hz, rotor frequency is about 0.5 Hz at the nominal values of supply voltage, frequency and torque; because under normal running condition, the slip is around 1 %. (Only in countercurrent braking the slip is higher than 1 but such braking may only be used for very short periods of time). As a result, for this specific motor, rotor core loss caused by fundamental is ignored. Another constant loss was mechanical losses which in induction motors occur in bearings, rotor friction and fans (called as windage losses).

Concerning variable losses, their dependency on load is highly significant, it means once the load changes the current flowing in stator and rotor windings are varied. This current based on variable load, generates variable losses that are also called copper losses (Hasanuzzaman, 2010).

To understand hierarchy relationships of variable and fixed losses in induction machine, Figure 1.1 presents this relationship well. Reference (Electrical Concepts, 2016) indicated a clarified overview for variable and constant losses as presented in Figure 1.2. Predominantly, the crucial losses for an induction motor [approximately 80% of total losses] are allocated to iron and copper losses (Kumar et al, 2010).

Based on a previous study (Zaheer et al, 2020) on this motor, the motor at its rated operating point generated electrical losses with the following shares: 41.5% of losses belong to stator joule losses, 26.5% to rotor joule losses and 31.8% to core losses. Since this motor is small, high winding resistances cause higher copper losses. In further section, deeper examinations on various losses for this motor are applied.

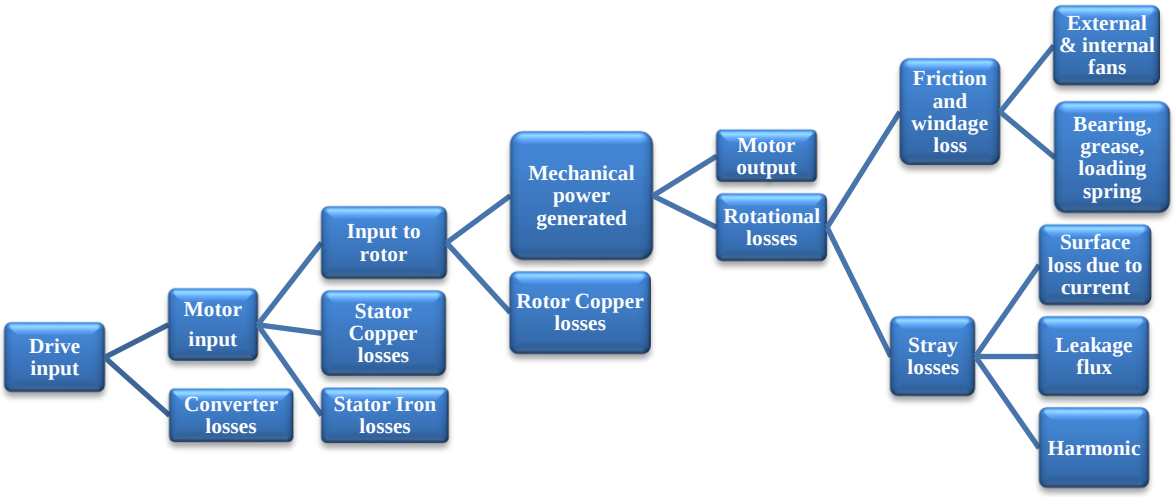

Figure 1.1. Hierarchy relationships of variable and fixed losses in an electrical drive.

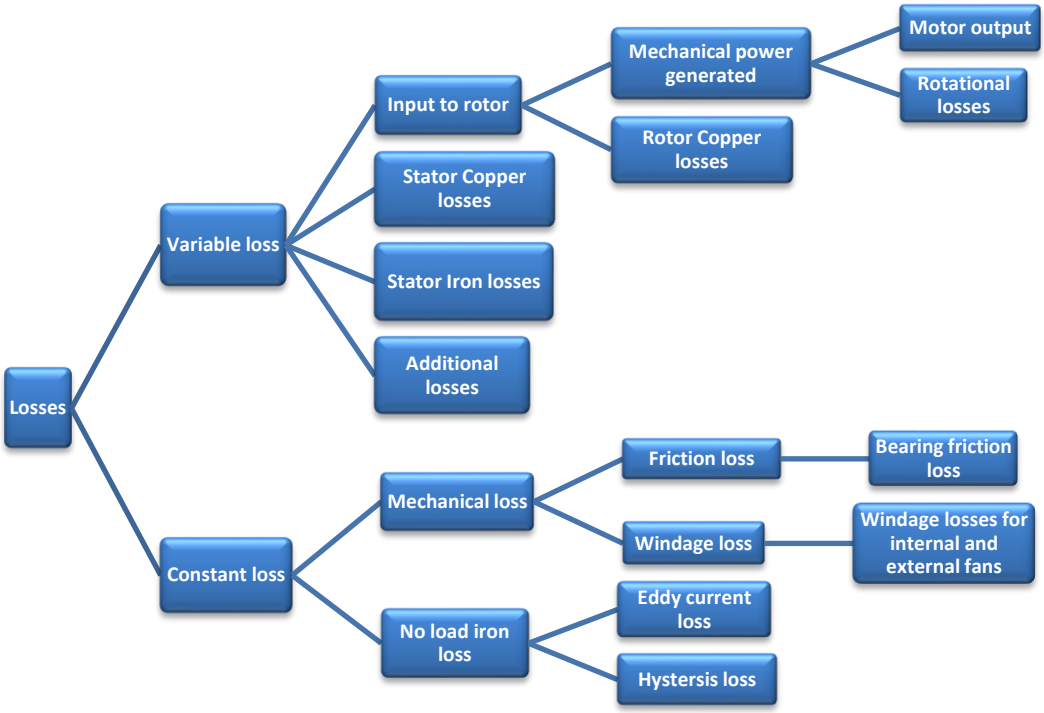

Figure 1.2. Category of losses in induction machine.

2 MULTIDISCIPLINARY MODELLING

The meaning of multidisciplinary modelling is to combine different computation models to establish a comprehensive model to include electromagnetic, mechanical, thermal, and fluid dynamics models as presented in Figure 2.1. In this Master's thesis, the electromechanical model was emphasized. The idea for the all-inclusive model states "there is irrefrangible relationship among these already mentioned models". In other words, the torque derived from the electromagnetic model is applied in the mechanical model. Then the mechanical model computes the rotor speed. Loss components taken from the electromechanical model are employed in a thermal model calculating which temperature points in different parts of the motor will be accomplished. Next a fluid dynamics model determines the cooling power needed for the motor based on imposed environmental temperature. In this section, a short introduction for each model and their relationships with another models is explained.

At this spot, the strong connections of each model intertwined to each one are well elucidated. In further, LUT Electrical Machines and Drives department aims to combine all models in order to include all-embracing model containing loss predication, rotor speed prediction, heat dissipation on each part of the motor and cooling system design for the motor.

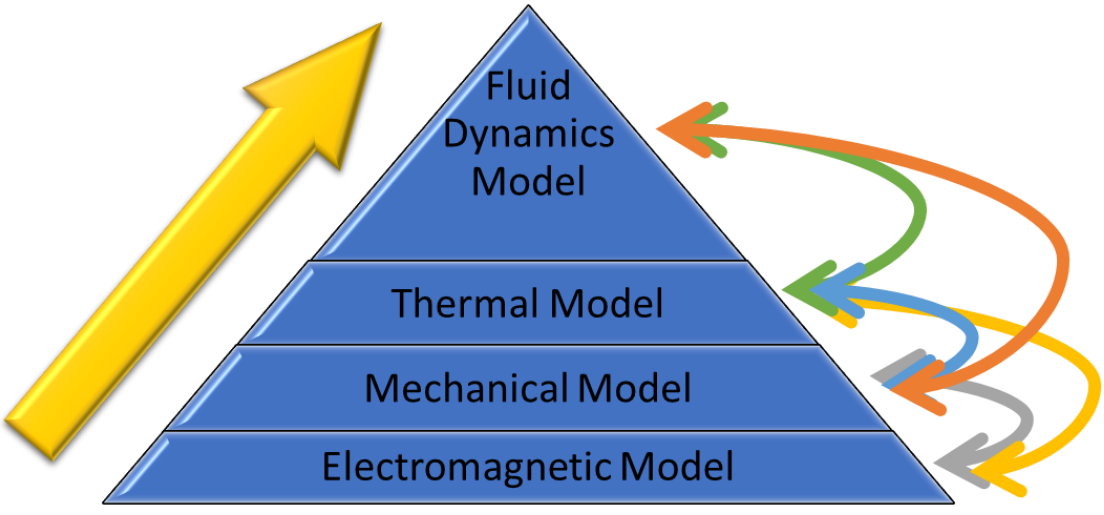

Figure 2.1. Model priorities of an integrated model for a motor.

2.1 Electromagnetic Model and Mechanical Model

Figure 2.2 illustrates one example how the coupling of the electromagnetic model and mechanical model can be simulated by (Aroua 2015). Rotational speed [dependent on frequency] and radial displacement [dependent on slip] are applied in the magnetic model and the electric model. In return, the electric model will deliver the calculated torque to the mechanical model.

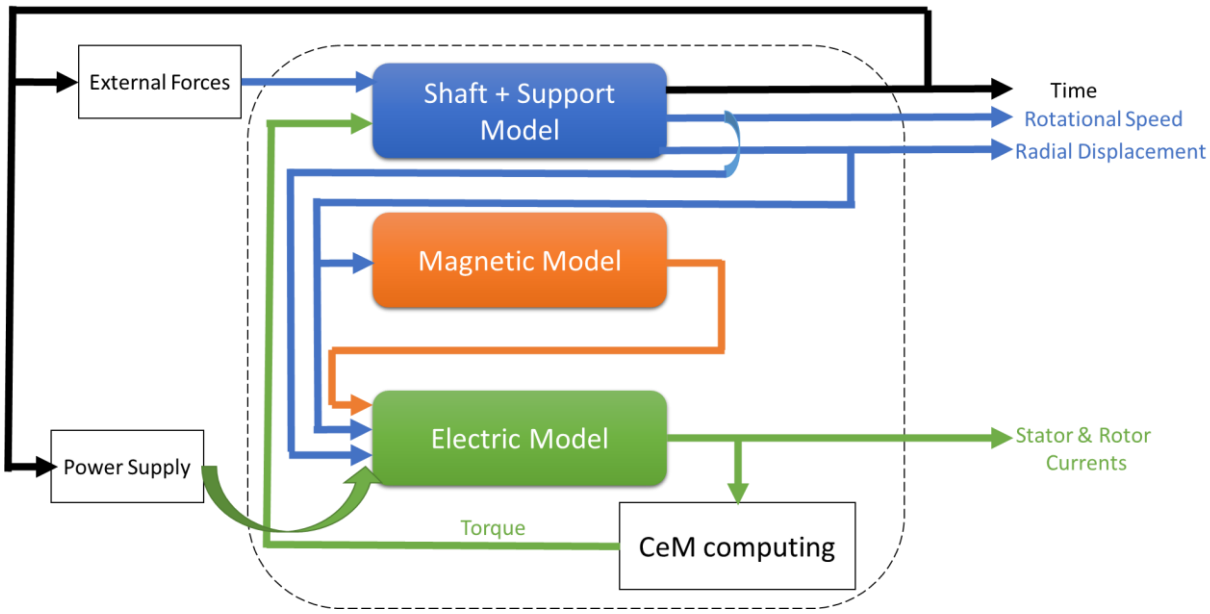

Figure 2.2. Coupling of electromagnetic model and mechanical model (Aroua, 2015).

2.2 Coupling of Thermal Model with other Models

In general, the total losses in electrical machines are split into losses of mechanical, magnetic, and electric losses. In Figure 2.3, the connection between the temperature dependency upon already-mentioned losses is illustrated. Obviously, all losses [electromagnetic and mechanical losses] appear in a form of heat energy (Schützhold and Hofmann, 2013).

1. Electric lossess

Winding losses or in other words, electric losses P_{E} in motors are gained via the equation below:

$$P_{\mathrm{E}} = 3R_{\mathrm{S}}{I_{\mathrm{S,rms}}}^2 + 3R_{\mathrm{R}}{I_{\mathrm{R,rms}}}^2, \tag{2.1}$$

Where, R_{S} and $I_{\mathrm{S,rms}}$ are the stator winding resistance and (RMS) root mean square value of the current flowing in stator winding. Since the machine is an induction motor, the rotor carries its own winding, therefore R_{R} and $I_{\mathrm{R,rms}}$ are rotor winding resistance and the rms value of the current running in the rotor winding. In metallic materials, the electric resistance faces a linear

rise with temperature T. T_0 is a reference temperature starting with initial resistive of R_0. α is the temperature coefficient of the material used.

$$R = R_0(1 + \alpha\,(T - T_0)), \tag{2.2}$$

2. Magnetic losses

As previously stated, two main parts of the iron stator core losses are hysteresis P_{hyst} and the eddy current P_{eddy} losses. These iron losses can be acquired by subtracting between the total losses and the copper losses. Based on reference (Xue et al, 2018), loss coefficients of eddy current and hysteresis losses are directly affected by frequency, flux density and temperature. Even temperature can solely intervene with these loss coefficients, if other parameters are considered the same constant values. All in all, role of temperature in iron loss coefficients are illustrated as below:

$$k_{\mathrm{h}}(T, f, B_{\mathrm{m}}) = k_{\mathrm{th}}(T, f, B_{\mathrm{m}})k_{\mathrm{h,T_0}}(f, B_{\mathrm{m}})$$
$$k_{\mathrm{e}}(T, f, B_{\mathrm{m}}) = k_{\mathrm{te}}(T, f, B_{\mathrm{m}})k_{\mathrm{e,T_0}}(f, B_{\mathrm{m}})$$

In which $k_{\mathrm{te}}(T, f, B_{\mathrm{m}})$ and $k_{\mathrm{th}}(T, f, B_{\mathrm{m}})$ are respectively temperature dependent coefficients of eddy current and hysteresis losses. With the initial temperature of T_0, these already introduced coefficients are developed in forms of $k_{\mathrm{e,T_0}}(f, B_{\mathrm{m}})$ and $k_{\mathrm{h,T_0}}(f, B_{\mathrm{m}})$. variable f and B_{m} are frequency and maximum value of alternating flux density.

3. Ventilation and friction losses

In bearings of rotor, friction losses appear that can be lessened with higher temperature that causes lower viscosity of lubricate. Besides, ventilation losses will be present if the machine owns a fan. The inner ventilation losses between the rotor and the stator are commonly negligible at standard motor speeds.

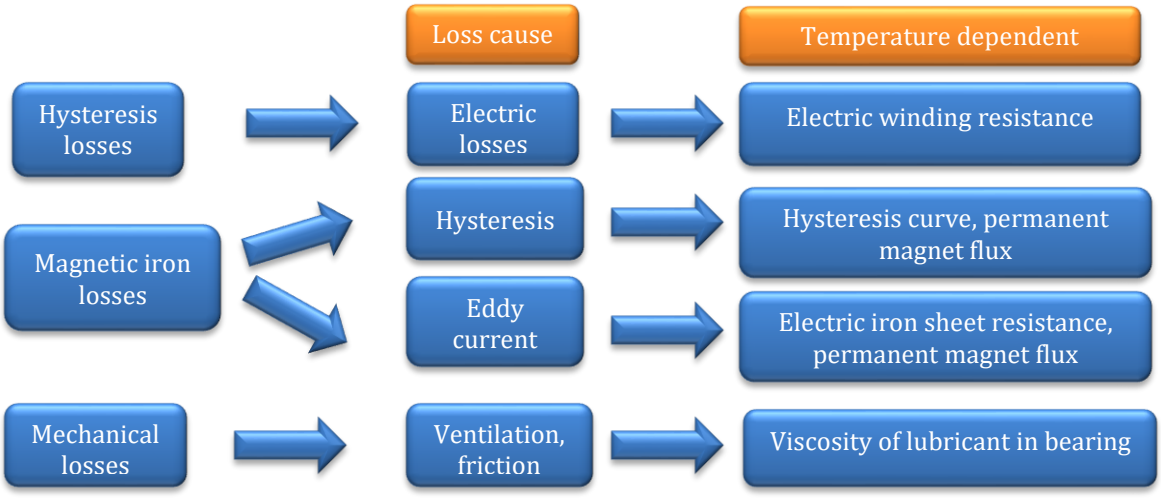

Figure 2.3. Role of temperature on various losses happening in induction motor (Schützhold and Hofmann, 2013).

2.3 Coupling of Fluid Dynamic Model with Other Models

The fluid dynamic computation results are the initial sign of the cooling potential of electrical machine. Generally, a model of fluid flow is presented by two basic approaches, namely lumped parameter method and CFD [Computational Fluid Dynamic] methods (Pechanek et al, 2015).

The temperature rise is main dimensioning principle in an electrical machine. The overheating is a serious issue in electrical machine, since it will be followed by disadvantages such as lower efficiency of motor, lower rated power, detrimental effect on insulation of motor which lead to a short operational lifetime. As an example of one CFD model, various parts of an induction motor around air gap were indicated in (Xie, Guo, Chen and Li, 2018). Table 2.1 shows the boundary conditions of computational fluid dynamic (CFD) computation in an induction motor. Here, the connection between the CFD model with other models can be witnessed with dependency with other models (Xie, Guo, Chen and Li, 2018).

Table 2.1. Boundary conditions of CFD model with other models (Xie, Guo, Chen and Li, 2018)

Boundary	**Condition**	**Model Dependency**
Stator inner wall	Stationary wall > No Slip	Thermal Model
Rotor outer wall	Stationary wall > No Slip	Thermal Model
Interface	Interface	Thermal Model
Rotating fluid domain	Angular Velocity > [Slip and frequency]	Mechanical Model

3 INDUCTION MOTOR PRINCIPLE

Before introducing the loss calculating tool, basic structure introduction for squirrel cage induction motor is required. Since the physical characteristics of the specific motor 5 kW will be discussed in this section, a general structure introduction for this motor is indispensable. The major parts of a simple AC motor are stator frame, stator core, rotor, windings and two end-shields.

There is a gap between the stator and rotor that is known as air gap. The magnitude of the air gap can drastically impact the motor performance. A large size of air gap causes an increased need of magnetizing current. On the other hand, a very tiny air gap leads to some troubles related to mechanical issues along with possible noise (Eslamian, 2016).

Outer stator frame

The outer frame is, naturally, dependent on the volume of the active parts of a motor. The responsibility of this frame is to sustain the stator core and shelter the inner parts of the machine (Circuit Globe, 2016).

Stator core

The prime duty of the stator magnetic core is to transfer the alternating magnetic field that generates hysteresis and eddy current losses. The stator stamping thickness is typically alternated between 0.3 mm and 0.5 mm. Protrusions embedded on the inner side of the stampings are called teeth and grooves of inner side are named slots (Circuit Globe, 2016).

Rotor construction

A laminated cylindrical core is a major part of a squirrel cage rotor. A hefty ring of copper or aluminum short each slot bar electrically. Slots are filled with uninsulated bar conductors made from copper or aluminum [In case of this Master's thesis, the specific rotor winding was made from aluminum]. It is worth to mention that the rotor slots are occasionally not in parallel to shaft but are skewed. This feature brings some benefits such as reducing the magnitude of the air-gap harmonics that reduces the noise and vibration in the machine (Circuit Globe, 2016).

Thus far the main parts of induction motor were illustrated, now the machine parameters of the motor are represented in table 3.1. The elementary characteristics of this three-phase induction motor are given in the table via Technical Specification of the motor.

Table 3.1. Machine Parameters.

Parameter	Variables	Value
Stator stack length [core length]	l (mm)	160
Stator core external diameter	D_{se} (mm)	220
Stator core inner diameter	D_s (mm)	125
Air gap	δ (mm)	0.5
Rotor core outer diameter	D_r (mm)	124
Winding configuration	-	Y
Rated RMS line to line voltage,	U_{LL} (V)	400
Rated frequency	f (Hz)	50
Rated speed	n_r (r/min)	1467
Rated power	P_n (kW)	5
Rated RMS current	I_s (A)	10.4
Number of winding turns in one phase	N_s	128
Number of stator slots	Q_s	48
Number of rotor slots	Q_r	40
Number of pole pairs	p	2
Number of parallel branches	a	2
Stator slot pitch	τ_{us} (mm)	8.1812
Stator pole pitch	τ_p (mm)	98.1748
Referring factor	p_v	4230
Rotor slot pitch	τ_{ur} (mm)	9.7389

4 LOSS MODELLING OF AN INDUCTION MOTOR

Previously, a short introduction regarding the loss categories was denoted. At this moment, more details will be distributed regarding each individual loss and its calculation. In this Master's thesis, an attempt was done to investigate the magnitude of several losses based on various conditions of working mode [partial and rated load] of an induction motor driven with a converter. The structure of the computation model is in Figure 4.1 below. The computations are written with MATLAB to establish an electric motor model. This MATLAB m-file script calculating tool can be found in Appendix 3 in this Master's thesis. The step numbers of Figure 4.1 are matched with m-file script section numbers written in Appendix 3.

The aim of this Master's thesis is to examine how the magnitude of losses were calculated through this tool. In Figure 4.1, the number of steps of the calculating tool can be found on each block. The Orange blocks mean they are directly affected by input values on the left-hand side and the green blocks indicate that they are independent of those input values.

Figure 4.1. Calculation procedure of the tool.

As Figure 4.1 shows the loss and efficiency computations are performed on the last step of 28. The already mentioned losses in prior sections are listed here and the way they were calculated, will be meticulously described. If the design of this tool had mattered here, the description order

should have started from step 1 and would have ended up in the last step of 28; however, this Master's thesis is planned to describe the way that each loss was attributed. Because of this interpretation, the explanation direction of each loss begins from the last step of 28 towards the beginning steps which contains the elementary requirements per loss computation. All equations introduced in this section were collected from (Pyrhönen et al, 2014).

4.1 Iron Loss

Iron loss (also termed as core losses) is occasionally generated in the stator teeth and yoke and in the rotor yoke. Iron loss can be the most significant loss, once field weakening operation is performed in traction machines. Stator iron loss P_{Fes}, is a function of stator voltage and frequency (Karlovsky et al, 2020). The stator iron loss P_{Fes} is majorly considered and the rotor iron loss is rather ignored. In high-speed machines, the iron losses in the rotor is contemplated high; however, in this 5 kW prototype motor since the rated synchronous speed is 1500 rpm, the iron losses are negligible.

The iron losses can be calculated by applying the equations (4.1), (4.2) and (4.3) which in order are core loss in the stator yoke, core loss in stator tooth and total iron losses in stator. Most of the variables in equations were defined in Table 4.1.

P_{15} is the material specific value of the losses of the material in unit W/kg along with peak flux density of 1.5 T and frequency of 50 Hz. Equations (4.1), (4.2) and (4.3) are practical for the rated frequency (50 Hz only) in the tool (Pyrhönen et al, 2014). Since the circumstance for modelling includes various conditions in different ranges of frequencies, equation (4.4) was applied for iron loss's estimations. There m, E_{m}, R_{Fe} are number of phases, air gap voltage and core loss resistance respectively (Bilal, 2020). It is worth to note that equations (4.1), (4.2) and (4.3) were employed to accomplish core loss resistance R_{Fe},which is afterwards used in equation (4.4).

$$P_{\mathrm{Fe,ys}} = k_{\mathrm{Fe,yoke}} P_{15} \left(\frac{\hat{B}_{\mathrm{ys}}}{1.5\ \mathrm{T}}\right)^2 m_{ys} \left(\frac{f}{50}\right)^{\frac{3}{2}}, \tag{4.1}$$

$$P_{\mathrm{Fe,ds}} = k_{\mathrm{Fe,tooth}} P_{15} \left(\frac{\hat{B}_{\mathrm{ds}}}{1.5\ \mathrm{T}}\right)^2 m_{\mathrm{ds,loss}} \left(\frac{f}{50}\right)^{\frac{3}{2}}, \tag{4.2}$$

$$P_{\mathrm{Fe}} = P_{\mathrm{Fe,ys}} + P_{\mathrm{Fe,ds}}\ , \tag{4.3}$$

$$P_{\mathrm{Fe}} = m\left(\frac{|E_{\mathrm{m}}|}{R_{\mathrm{Fe}}}\right)^2, \tag{4.4}$$

Table 4.1. Iron loss calculation parameters.

Parameter	Variable	Value
Stator teeth correction coefficient	$k_{\mathrm{Fe,tooth}}$	1.8
Stator yoke correction coefficient	$k_{\mathrm{Fe,yoke}}$	1.6
Space factor of stator and rotor core	k_{Fe}	0.97
Specific loss at (1.5 T, 50 Hz)	P_{15} (W/kg)	6.74
Density of iron	ρ_{fe} kg/m^3	7600

4.1.1 Investigation of core loss resistance on iron loss

Equation (4.4) in the tool was utilized by two attempts in the tool. The first attempt was made to find R_{Fe} with the help of equation (4.3) in form of equation (4.5) below and then the second attempt was performed to find the stator iron loss in form of (4.4) itself. The difference for the second attempt is the induced air gap voltage E_{m} which was inserted based on the rotor speed, unlike the first attempt that this induced air gap voltage was independent of input rotor speed.

$$R_{\mathrm{Fe}} = m\left(\frac{|E_{\mathrm{m}}|}{P_{\mathrm{Fe}}}\right)^2, \tag{4.5}$$

4.1.2 Investigation of air gap voltage on iron loss

As stated previously, two different statuses for variable E_{m} were assigned. Initially E_{m} depending the rotor speed and then E_{m} heedless of the rotor speed.

E_{m} based on input rotor speed:

In the first condition, E_{m} is available. U_{Phase} is a phase voltage.

$$E_{\mathrm{m}} = U_{\mathrm{Phase}} - I_{\mathrm{s}}Z_{\mathrm{s}}\ , \tag{4.6}$$

Z_{s} is stator circuit impedance that was attained in step number 26 regardless of any input rotor speed. I_{s} is stator current that depends on rotor speed that is acquired as below:

$$I_{\mathrm{s}} = \frac{U_{\mathrm{Phase}}}{Z}\ , \tag{4.7}$$

That Z is the total impedance of the equivalent circuit in step 26. Z_{m} below is magnetizing circuit impedance regardless of input rotor speed and $\acute{Z}_{\mathrm{r}}$ is rotor circuit impedance according to the rotor speed that was achieved with equation (4.9). s is the rotor per unit slip. In section 4.2.2, more information regarding equation (4.9) will be given.

$$Z = Z_{\mathrm{s}} + \frac{Z_{\mathrm{m}}\acute{Z}_{\mathrm{r}}}{Z_{\mathrm{m}}+\acute{Z}_{\mathrm{r}}}\,, \tag{4.8}$$

$$\acute{Z}_{\mathrm{r}} = \frac{\acute{R}_{\mathrm{r}}}{s} + j\acute{X}_{\sigma\mathrm{r}}, \tag{4.9}$$

$\acute{X}_{\sigma\mathrm{r}}$ or in other words $\acute{X}_{\mathrm{r}}$ and $\acute{R}_{\mathrm{r}}$ are rotor inductance and resistance referred to stator that in step 26 were accomplished. In step 17, this transformation ratio for IM impedance is in reached. Before multiplying by ρ_V, rotor resistance (without referred to stator) was calculated in the beginning of step 17. In section 4.3, more information about rotor resistance can be found.

$$\rho_{\mathrm{V}} = \frac{4m}{Q_{\mathrm{r}}}\left(\frac{N_{\mathrm{s}}k_{\mathrm{w1}}}{k_{\mathrm{sq}}}\right)^2, \tag{4.10}$$

Q_{r}, N_{s} are available in table 3.1 that were inserted in steps of 5, 8 of the calculating tool. Also k_{w1}, k_{sq} are fundamental winding factor and skewing factor obtained in steps of 7 and 17.

E_{m} based on rated rotor speed:

In step 7 and according to table 3.1, the air gap induced voltage was conveniently acquired via equation below. U_{LL} is input voltage given before running the tool.

$$E_{\mathrm{m}} = 0.94\left(\frac{U_{\mathrm{LL}}}{\sqrt{3}}\right)\,, \tag{4.11}$$

4.1.3 Investigation of maximum flux density and mass of stator yoke on iron loss

Now, it is time to discuss variables on equation (4.1). In equation (4.1), some parts of the variables were denoted in table 4.1. Based on reference (Pyrhönen et al, 2014), the maximum flux density in stator yoke $\hat{B}_{\mathrm{ys}}$ was given to the tool in step 14. As for the mass of the stator yoke m_{ys}, it was attributed in equation (4.12). V_{ys} is the volume of the stator yoke that was calculated in step 25. Other variables in equation (4.12) were given in table 4.1 and also in step number 1 in the tool.

$$m_{\mathrm{ys}} = V_{\mathrm{ys}}k_{\mathrm{Fe}}\rho_{\mathrm{Fe}}\,, \tag{4.12}$$

4.1.4 Investigation of maximum flux density and mass of stator teeth on iron loss

Equation (4.2) is as analogous with equation 4.1. The proper magnitude of $\hat{B}_{\mathrm{ds}}$ according to (Pyrhönen et al, 2014) was entered into the tool in step 12. In regard to stator teeth equation (4.13) demonstrates the computation. Q_{s} is the number of stator slots that is visible in table 3.1 and in step 5. b_{ds} is the stator tooth width calculated in step 10. $h_{5\mathrm{s}}$ is one of the dimensions of

stator tooth discussed in detail in step 11. l is the core length in the motor without cooling channels available in step 4 of the tool and in Table 3.1. $\rho_{\mathrm{Fe}}$is iron density faced on Table 4.1.

$$m_{\mathrm{ds,loss}} = k_{\mathrm{Fe}}\rho_{\mathrm{Fe}}Q_{\mathrm{s}}b_{\mathrm{ds}}h_{5\mathrm{s}}l\,, \tag{4.13}$$

4.2 Stator Copper Loss

Copper losses [also known as Joule losses] are divided into stator and rotor losses. Stator copper loss P_{cs} is primarily affected via torque and secondarily via stator voltage and frequency and then temperature. To attain the stator copper losses in a three-phase induction motor, equation (4.14) provides the magnitude, where R_{s} is stator resistance and I_{s} is stator current (Aarniovuori et al, 2019). Furthermore, a clarification concerning this rotor copper loss is given in Section 4.3.

$$P_{\mathrm{cs}} = mR_{\mathrm{s}}I_s^2, \tag{4.14}$$

Table 4.2. Stator copper loss calculation parameters.

Parameter	Variable	Value
Number of coil turns in series	N	128
Average length of a coil turn	$l_{\mathrm{av}}(\mathrm{m})$	0.4869
Copper conductivity (@100°C)	$\sigma_{\mathrm{c}}(\mathrm{MS/s})$	43.8
Cross sectional area of the stator slot	$S_{\mathrm{Cu,s}}(\mathrm{mm}^2)$	1.2039
Stator resistance	$R_{\mathrm{s}}(\Omega)$	0.5895

4.2.1 Investigation of stator resistance on stator copper loss

Stator resistance is attributed via the equation (4.15) in step 16. All components in this equation can be found in table 4.2 and table 3.1. It is worthy to note that stator resistance value was not inserted into the tool by equation 4.15 but also a DC stator resistance measurement done by LUT laboratory was utilized notwithstanding of input rotor speed and input frequency.

$$R_{\mathrm{s}} = \frac{Nl_{\mathrm{av}}}{\sigma_{\mathrm{cu}}aS_{\mathrm{cs}}}\,, \tag{4.15}$$

4.2.2 Investigation of stator current on stator copper loss

At this point, stator current is affected by input rotor speed, computed in step 27 of the tool and in equation (4.16). Actually, this dependency is coming from step 26 namely equivalent circuit parameters. Parameter Z is the total impedance of the equivalent circuit that is influenced by input frequency and rotor speed.

$$I_{\mathrm{s}} = \frac{U_{\mathrm{phase}}}{Z}\,, \tag{4.16}$$

$$Z = Z_{\mathrm{s}} + \frac{Z_{\mathrm{m}}\acute{Z}_{\mathrm{r}}}{Z_{\mathrm{m}}+\acute{Z}_{\mathrm{r}}}\,, \tag{4.17}$$

Z_{s} and Z_{m} are stator circuit and magnetizing circuit impedances that are independent of rotor speed. Then $\acute{Z}_{\mathrm{r}}$ is rotor circuit impedance upon input rotor speed that is credited as below:

$$\acute{Z}_{\mathrm{r}} = \frac{\acute{R}_{\mathrm{r}}}{s} + \mathrm{j}\acute{\mathrm{X}}_{\sigma\mathrm{r}}\,, \tag{4.18}$$

About $\acute{R}_{\mathrm{r}}$, the detail was given in section 4.3.1 and as for $\acute{\mathrm{X}}_{\sigma\mathrm{r}}$ equations below guide as following. ω is angular stator speed.

$$\acute{\mathrm{X}}_{\sigma\mathrm{r}} = \acute{\mathrm{X}}_{\mathrm{r}} = \acute{L}_{\mathrm{r}}\omega$$

$$\acute{L}_{\mathrm{r}} = p_{\mathrm{v}}\left(L_{\mathrm{bar}}K_{\mathrm{L}} + \frac{L_{\mathrm{ring}}}{2\sin\left(\frac{\pi p}{Q_{\mathrm{r}}}\right)^2}\right)\,, \tag{4.19}$$

In equation (4.19), K_{L} is the variable factor that based on input rotor speed is changed, L_{bar} is the rotor bar leakage inductance that was calculated its each component in several tool steps including steps: 24, 20, and 21. L_{ring} is rotor end winding leakage calculated in Step 24. Other parameters in the equation (4.19) has been introduced before.

The magnetizing circuit impedance Z_{m} in equation (4.17) is gained as below in step 26:

$$Z_{\mathrm{m}} = \frac{R_{\mathrm{Fe}}X_{\mathrm{m}}\mathrm{j}}{R_{\mathrm{Fe}}+X_{\mathrm{m}}\mathrm{j}}, \tag{4.20}$$

Regarding R_{Fe} more detail is available on Section 4.1.1. As for X_{m}, the magnetizing inductance in Step 18.

$$X_{\mathrm{m}} = L_{\mathrm{m}}\omega$$

$$L_{\mathrm{m}} = \frac{m}{2}\frac{2}{\pi}\mu_0\acute{l}\frac{1}{2p}\frac{4}{\pi}\frac{\tau_{\mathrm{p}}}{\delta_{\mathrm{ef}}}(k_{\mathrm{w1}}N)^2, \tag{4.21}$$

In equation 4.21, μ_0 is the permeability of vacuum and δ_{ef} is effective air gap witnessed in step 18. Other components for equation (4.21) have been presented before and were seen in Table 3.1. The effective air gap is achieved through equation below.

$$\delta_{\mathrm{ef}} = \frac{U_{\mathrm{m\delta e}}+U_{\mathrm{mds}}+U_{\mathrm{mdr}}+\frac{U_{\mathrm{mys}}}{2}+\frac{U_{\mathrm{myr}}}{2}}{U_{\mathrm{m\delta e}}}\delta_{\mathrm{e}}\,, \tag{4.22}$$

Elements applied in equation (4.22) are δ_{e}, $U_{\mathrm{m\delta e}}$, U_{mds}, U_{mdr}, U_{mys} and U_{myr} are in order equivalent air gap computed on Step 13, magnetic voltage of air gap calculated on Step 13,

magnetic voltage of stator tooth available on Step 12, magnetic voltage of rotor tooth attained on step 12, magnetic voltage of stator yoke determined on Step 14 and, magnetic voltage of rotor yoke intended on Step 14.

4.3 Rotor Copper Loss

Correspondingly, as for the rotor copper losses P_{cr}, I'_{r} is attributed as the rotor current of single-phase equivalent circuit referred to the stator and R'_{r} is the rotor resistance in the following equation (Aarniovuori et al, 2019). Rotor copper loss P_{cr}, is mainly functioned by torque, and minorly by the slip and temperature.

$$P_{\mathrm{cr}} = mR'_{\mathrm{r}}(I'_{\mathrm{r}})^2, \tag{4.23}$$

Table 4.3. Rotor copper loss calculation parameters.

Parameter	Variable	Value
Bar resistance	$R_{\mathrm{bar}}(\mathrm{m\Omega})$	0.1188
Rotor bar length	$l_{\mathrm{bar}}(\mathrm{mm})$	160
Aluminium conductivity (@100°C)	$\sigma_{\mathrm{Al}}(\mathrm{MS/s})$	27.7
Bar cross sectional area	$S_{\mathrm{bar}}(\mathrm{mm}^2)$	48
Length of SC-ring portion (mm)	$l_{\mathrm{ring}}(\mathrm{mm})$	7.6
Cross sectional area of SC-ring (mm)	$S_{\mathrm{ring}}(\mathrm{mm}^2)$	375
Referring factor	p_{v}	4230
Rotor resistance referred to stator	$\acute{R}_{\mathrm{r}}(\Omega)$	0.5659

4.3.1 Investigation of resistance rotor on rotor copper loss

First, DC resistance of rotor bar is examined as below in step 17:

$$R_{\mathrm{bar}} = \frac{l_{\mathrm{bar}}}{S_{\mathrm{bar}}\sigma_{\mathrm{Al}}}, \tag{4.24}$$

Also, resistance of rotor ring is:

$$R_{\mathrm{ring}} = \frac{l_{\mathrm{ring}}}{S_{\mathrm{ring}}\sigma_{\mathrm{Al}}}, \tag{4.25}$$

$$R_{\mathrm{r}} = R_{\mathrm{bar}} + \frac{R_{\mathrm{ring}}}{2\sin(\frac{\pi p}{Q_{\mathrm{r}}})^2}, \tag{4.26}$$

With help of equation (4.10) and equation (4.27), rotor resistance referred to stator in equation (4.28) is approachable.

$$\acute{R}_{\mathrm{r}} = p_{\mathrm{v}}R_{\mathrm{r}}, \tag{4.27}$$

In step 26, the variable rotor resistance referred to stator based on rotor speed is:

$$\acute{R}_{\mathrm{r}} = p_{\mathrm{v}}\left(R_{\mathrm{bar}}k_{\mathrm{R}} + \frac{R_{\mathrm{ring}}}{2\sin\left(\frac{\pi p}{Q_{\mathrm{r}}}\right)^2}\right), \tag{4.28}$$

That k_{R} is the variable based on rotor speed and other elements own fixed magnitudes.

4.3.2 Investigation of rotor current in rotor copper loss

Rotor current is attained based on input rotor speed in step 27 as following:

$$\acute{I}_{\mathrm{r}} = I_{\mathrm{s}}\frac{Z_{\mathrm{m}}}{Z_{\mathrm{m}}+\acute{Z}_{\mathrm{r}}}, \tag{4.29}$$

In equation (4.29), I_{s} and $\acute{Z}_{\mathrm{r}}$ are varied based on input rotor speed and Z_{m} includes its constant amplitude regardless of magnitude of input rotor speed. Regarding I_{s} more details are accessible in section 4.1.2. Concerning $\acute{Z}_{\mathrm{r}}$, equation (4.18) illustrates more information.

4.4 Mechanical Loss

The mechanical losses appear via the friction in the rotor bearings and to the forced ventilation air within the motor structure, where the mechanical power is wasted in form of heat in the bearings roller elements (Sousa et al, 2012). In this Master's thesis equation (4.30) was applied for mechanical losses in bearings and windage losses in step 25. In order $k_{\mathrm{p.}}$,$D_{\mathrm{r.}}$, l, τ_p, v_{r} are experimental factors for windage and bearing losses, rotor diameter, core length in the machine, stator pole pitch, and velocity. The already mentioned variables were inserted into the tool by the step order of 25, 3, 5, and 25. Regarding the total mechanical losses P_{mech}, equation (4.31) was employed that n_{r} is rotor speed and n_{s} is synchronous speed.

$$P_{\mathrm{fw}} = k_{\mathrm{p}}D_{\mathrm{r}}(l + 0.6\tau_{\mathrm{p}}){v_{\mathrm{r}}}^2, \tag{4.30}$$

$$P_{\mathrm{mech}} = P_{\mathrm{fw}}\left(\frac{n_{\mathrm{r}}}{n_{\mathrm{s}}}\right)^3, \tag{4.31}$$

Table 4.4. Mechanical loss calculation parameters

Parameter	Variable	Value
Rotor diameter	D_{r} (m)	0.124
Experimental factor for windage and bearing	k_{p} ($\mathrm{Ws^2/m^4}$)	15
Stator pole pitch	τ_{p}	0.0982

4.5 Stray Loss

Stray loss P_{st} or in other words, additional load loss, is the most mysterious loss among other well-known losses that there are many methods to calculate its magnitude. Additional losses can appear in the air gap once field distribution in form of sinusoidal waveforms exist. Even in stator slots and conductors, additional losses can emerge by induced skin effect. Stray loss is primarily associated to torque, and is secondarily linked to frequency, temperature, and stator voltage. In the tool, equation (4.32) was implemented for this loss available on reference (Kärkkäinen, 2015). Here A, B and T are linear regression constant [slope], linear regression constant [value at zero] and torque.

$$P_{\mathrm{st}} = A \cdot T^2 + B, \tag{4.32}$$

4.6 Harmonic losses

When an electrical machine is driven with a converter, an additional loss component is formed in magnetic fields which contain numerous time harmonics of power supply that these losses are generated by rotor slot ripple, phase band and stator. Harmonic losses were made through these time harmonic field in different parts of machine including rotor conductor, stator windings, and rotor and stator cores (Yamazaki, 2003). Harmonic loss was not considered into this tool.

4.7 Total Losses and Efficiency

The total loss by adding all previous defined losses is at reach with equation (4.33):

$$P_{\mathrm{total}} = P_{\mathrm{st}} + P_{\mathrm{cs}} + P_{\mathrm{cr}} + P_{\mathrm{Fe}} + P_{\mathrm{mech}}\ , \tag{4.33}$$

The input power is known; however, for output power in step 27, equation (4.34) was used:

$$P_{\mathrm{out}} = m(\left|\acute{I}_{\mathrm{r}}\right|)^2 \frac{1-s}{s} \acute{R}_{\mathrm{r}} - P_{\mathrm{mech}}\ , \tag{4.34}$$

The parts of equation (4.34) were previously defined and also, they are affected by input rotor speed. Subsequently the efficiency can be discovered:

$$\eta = \frac{P_{\mathrm{out}}}{P_{\mathrm{in}}} = \frac{P_{\mathrm{out}}}{P_{\mathrm{out}} + P_{\mathrm{total}}}\ , \tag{4.35}$$

5 COMPARISON TO MEASURED RESULTS

At this stage, computation model results are verified with experimental results of the 5 kW induction motor. The principal values of the motor are previously introduced in Chapter 3, Table 3.1. The studied 5 kW motor was measured in laboratory at different load and speed conditions to verify the accuracy of the designed computation model. To examine the predication potential of this tool, 24 operating points were compared with real losses measured in LUT lab with a fully controllable generator supply. Table 5.1 indicates the motor operating points. In Appendix 1, the initial values inserted for this comparison are available.

The model is capable of predicting the power factor, stator impedance, rotor impedance, and maximum torque during the various rotor speeds and torques [refer in Appendix 2]. The loss segregation method based on IEC 60034-2-1 standard was utilized in the measurements (IEC 60034-2-1, Lindh 2018). At five loading conditions [from under rated load to overload] with respect to their required voltage and frequency, were utilized in the tool and the result in form of contour diagrams, Figures 5.1 – 5.7, were exemplified.

Table 5.1. Various operation conditions used with designed loss calculation model.

Input Voltage Magnitude Per Condition [V]		**Frequency [Hz]**			
		12.5	**25**	**37.5**	**50**
***T* (%)**	**125**	100	200	300	400
	115	100	200	300	400
	100	100	200	300	400
	75	100	200	300	400
	50	100	200	300	400
	25	100	200	300	400

The analytical findings appeared near actual measured data on a satisfactory boundary. The total loss comparison, Figure 5.1, in lower frequency embodied a better similarity with analytical and experimental results, while the input frequency approaches to its rated magnitude

less accuracy in comparison emerges. The measured values are different because the modulation and loss of voltage which were not considered in the right-hand side figure.

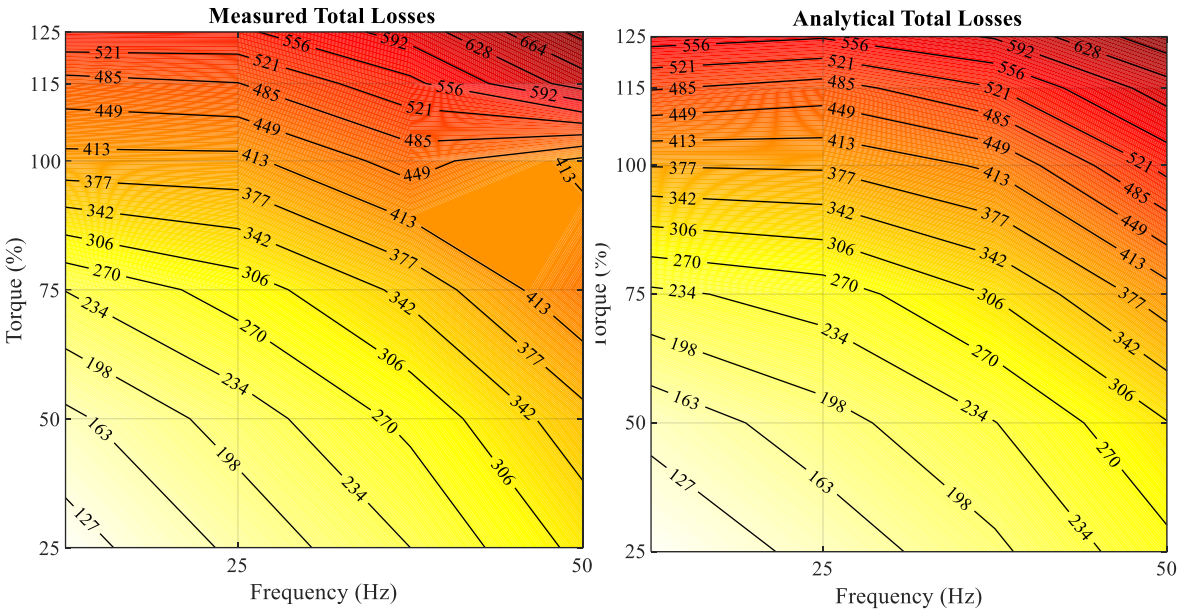

Figure 5.1. Measured and calculated motor losses (unit in W).

Although some minor deviations occurred in the loss comparison, the efficiency, depicted in Figure 5.2, looks precise in comparison. This is due to different output power in analytical and experimental results.

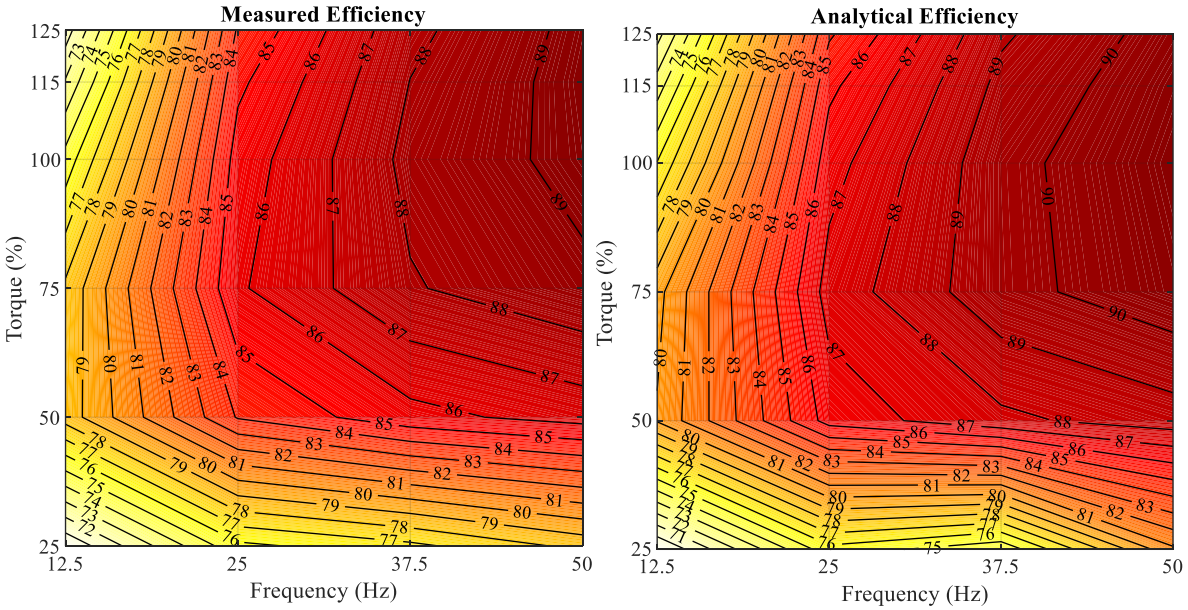

Figure 5.2. Comparison of measured and calculated efficiency.

In this comparison, most of the deviations belong to mechanical losses shown in Figure 5.3. Predicating this loss is immensely demanding. It is even difficult to measure it experimentally. Since the share of this loss is low, it could not affect drastically on the total results.

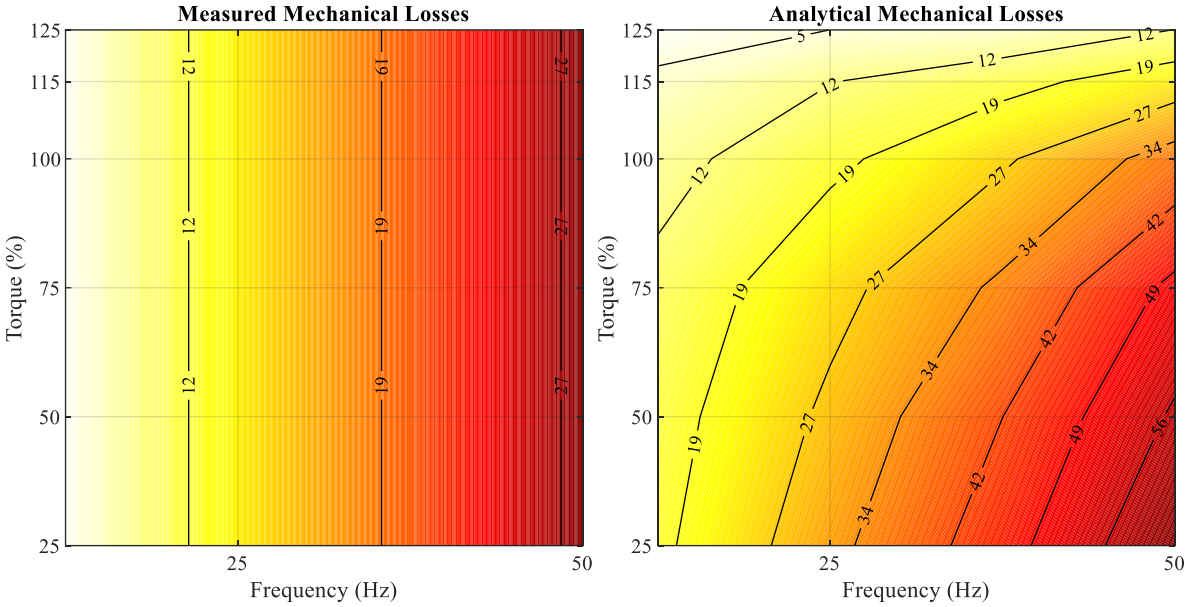

Figure 5.3. Comparison of measured and calculated mechanical losses (unit in W).

Additional loss comparison looks extremely promising, this is due to the experimental equation in Section 4.5. Since predicting this loss was truly challenging, with help of this equation, a proper evaluation scale between analytical and experimental result was carried out.

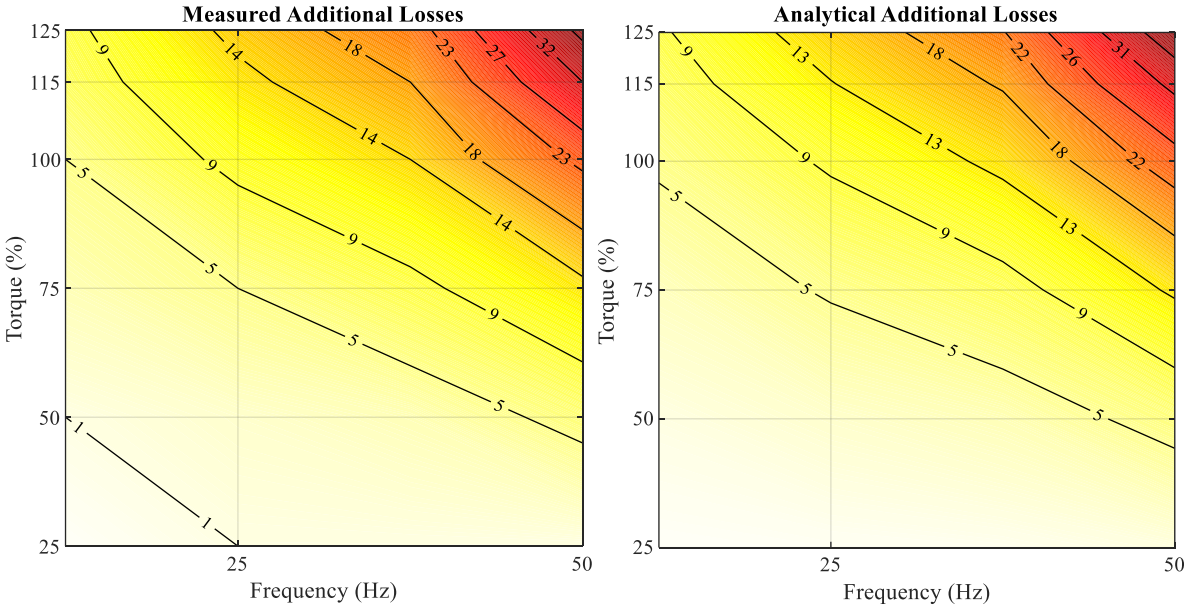

Figure 5.4. Comparison of measured and calculated additional losses (unit in W).

Iron losses and copper losses in the stator and rotor are fairly reached to expectations in all

operating points as depicted in the Figures 5.5 - 5.7.

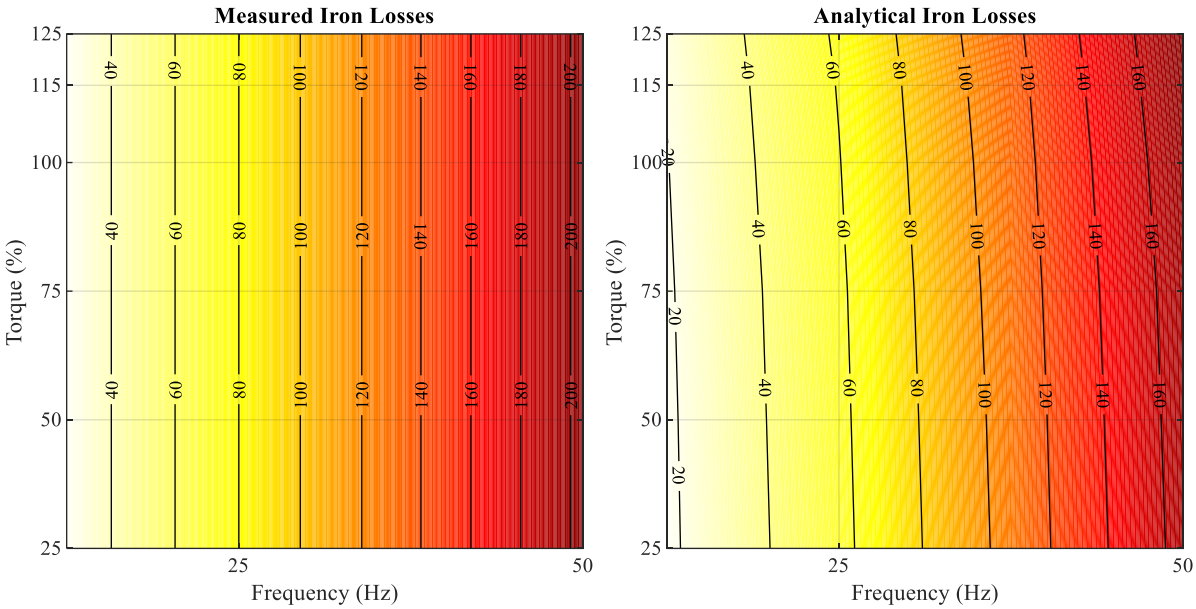

Figure 5.5. Comparison of iron losses calculation (unit in W).

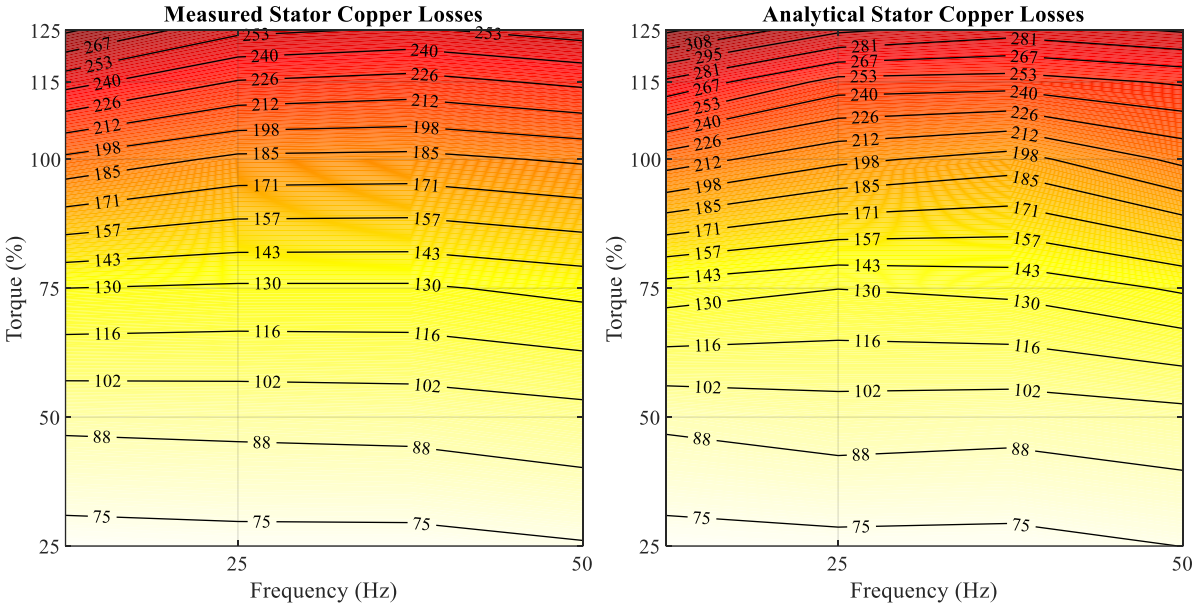

Figure 5.6. Comparison of stator copper losses calculation (unit in W).

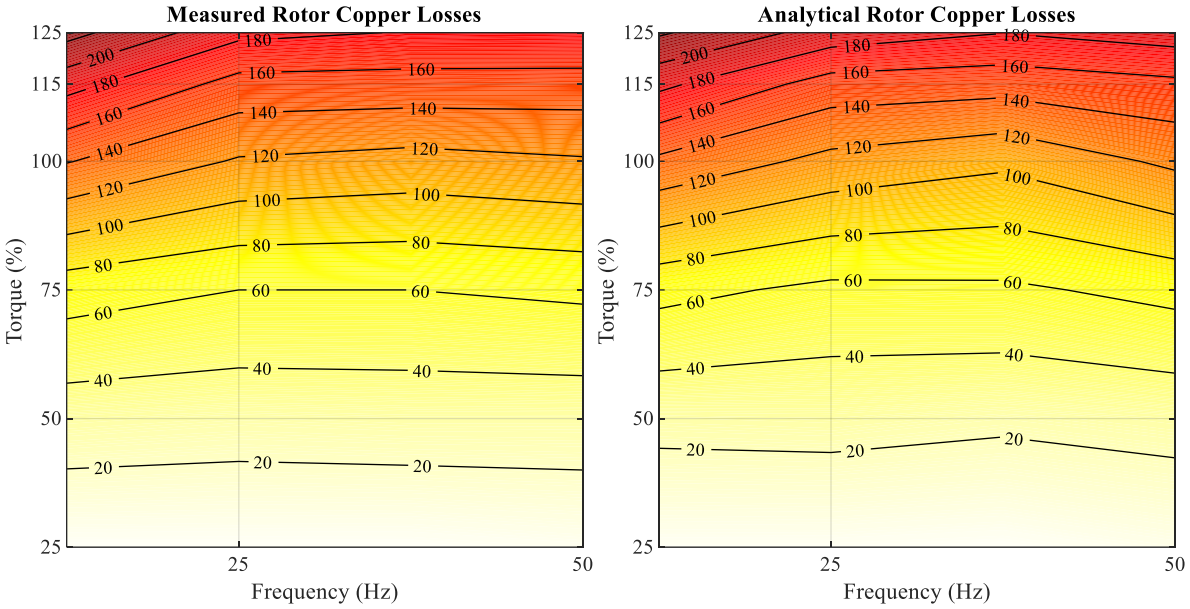

Figure 5.7. Comparison of rotor copper losses (unit in W).

6 CONCLUSIONS

The analytical loss calculation model itself can be independent if the need for comparison is not essential. In this case, experimental values measured in LUT laboratory were available. An analytic loss calculation tool was developed and used to compare calculated and measured losses with each other. This comparison can aid to spot any disparities with the design values assigned in the tool. The Loss Calculating model demonstrated satisfactory accuracy. Apart from the result for various results, the model is capable of computing the maximum torque, power factor, stator and rotor impedance and also feasible value for efficiency. The deviation of data comparison between analytical and measured values is mainly caused by mechanical losses that seem very tricky to be calculated analytically and measure experimentally. This model is supposed to be later upgraded to estimate heat losses further on behalf of LUT laboratory.

REFERENCES

Aarniovuori, L., Lindh, P., Kärkkäinen, H., . Niemelä, M., Pyrhönen, J., and Cao, W., "Analytical Evaluation of High-Efficiency Induction Motor Losses," 2019 IEEE International Electric Machines & Drives Conference (IEMDC), San Diego, CA, USA, 2019, pp. 1501-1507, doi: 10.1109/IEMDC.2019.8785380.

Aroua. FOURATI, "An electromagnetic-mechanical modeling of an induction motor and rotor shaft coupled to angular approach", 22 eme Congres Francais de Mecanique, 24, 28, 2015.

Bilal, N. (2020). An Accurate Iron Core Loss Model in Equivalent Circuit of Induction Machines. Journal of Energy. 2020. 1-10. 10.1155/2020/7613737.

Cao-Minh Ta and Hori, Y., 2001. Convergence improvement of efficiency-optimization control of induction motor drives. IEEE Transactions on Industry Applications, 37(6), pp.1746-1753.

Choudhary, P., Dubey, S. and Gupta, V., 2015. Efficiency Optimization of Induction Motor Drive at Steady-State Condition. ICCICCT,.

Circuit Globe. 2016. *Construction Of Induction Motor - Circuit Globe*. [online] Available at: <https://circuitglobe.com/construction-of-induction-motor.html> [Accessed 14 February 2020].

Electrical Concepts. 2016. Stray Load Loss And Mechanical Loss In An Electrical Machine | Electrical Concepts. [online] Available at: <https://electricalbaba.com/stray-load-loss-and-mechanical-loss-in-an-electrical-machine/> [Accessed 1 June 2020].

Eslamian, M. (2016). Technical Language for Power Electric Technician Students. 10.13140/RG.2.2.17658.70084.

Hasanuzzaman, M., Rahim, N.A., Saidur, R., Kazi, S.N., Energy savings and emissions reductions for rewinding and replacement of industrial motor, Energy, Volume 36, Issue 1, 2011, Pages 233-240, ISSN 0360-5442

IEC 60034-2-1, Rotating electrical machines – Part 2-1: Standard methods for determining losses and efficiency from tests (excluding machines for traction vehicles), Ed. 2, IEC 60034-2-1, June 2014.

Karlovsky, P.; Lipcak, O.; Bauer, J. Iron Loss Minimization Strategy for Predictive Torque Control of Induction Motor. Electronics 2020, 9, 566.

Kumar, K., Sakthibala, D. and Palaniswami, D., 2010. Efficiency Optimization of Induction Motor Drive Using Soft Computing Techniques. *International Journal of Computer Applications*, 3(1), pp.6-12.

Pechanek, R., Kindl, V. and Skala, B., 2015. TRANSIENT THERMAL ANALYSIS OF SMALL SQUIRREL CAGE MOTOR THROUGH COUPLED FEA. *MM Science Journal*, 2015(01), pp.560-563.

Pyrhönen, J., Jokinen, T. and Hrabovcová, V., 2014. Design Of Rotating Electrical Machines. Chichester: Wiley, Second Edition.

Lindh, P, Lassi Aarniovuori, Hannu Kärkkäinen, Markku Niemelä and Juha Pyrhönen, “IM motor loss evaluation using FEA and measurements,” XXIII International Conference on Electrical Machines (ICEM), 2018

Sousa, K., Hafner, A., Kalinowski, H. and da Silva, J., 2012. Determination of Temperature Dynamics and Mechanical and Stator Losses Relationships in a Three-Phase Induction Motor Using Fiber Bragg Grating Sensors. IEEE Sensors Journal, 12(10), pp.3054-3061.

Schützhold, J. and Hofmann, W., 2013. Analysis of the Temperature Dependence of Losses in Electrical Machines. *IEEE*,.

Xie, Y., Guo, J., Chen, P. and Li, Z., 2018. Coupled Fluid-Thermal Analysis for Induction Motors with Broken Bars Operating under the Rated Load. *Energies*, 11(8), p.2024.

Xue, S., Feng, J., Guo, S. et al. (3 more authors) (2018) A New Iron Loss Model for Temperature Dependencies of Hysteresis and Eddy Current Losses in Electrical Machines.IEEE Transactions on Magnetics, 54 (1). 8100310. ISSN 0018-9464

Yamazaki, K. "Torque and efficiency calculation of an interior permanent magnet motor considering harmonic iron losses of both the stator and rotor," in *IEEE Transactions on Magnetics*, vol. 39, no. 3, pp. 1460-1463, May 2003, doi: 10.1109/TMAG.2003.810515.

Zaheer, M,. Lindh, P,. Aarniovuori, L,. Pyrhönen, J,. (2020). Assessment of 5 kW Induction Motor Finite element computations with a Commercial and an Open-source software. 10.1109/ACEMP-OPTIM44294.2019.9007150.

APPENDICES

Appendix 1

The initial measured values applied in the analyzing model.

Table I. Measured rated torque of the 5 kW Induction Motor (Nm)

	f (Hz)			
T (%)	**12.5**	**25**	**37.5**	**50**
125	42.10	40.76	40.43	40.64
115	38.74	37.55	37.22	37.43
100	**33.58**	**32.60**	**32.31**	**32.53**
75	24.93	24.13	23.93	24.27
50	16.52	15.97	15.88	16.26
25	7.84	7.58	7.53	8.02

Table II. Measured rotor speed of the 5 kW Induction Motor (rpm)

	f (Hz)			
T (%)	**12.5**	**25**	**37.5**	**50**
125	325	707	1084	1458
115	330	712	1088	1462
100	**337**	**717**	**1094**	**1466**
75	349	727	1102	1475
50	359	734	1110	1484
25	368	743	1119	1491

Table III. Measured temperature rise in stator of the 5 kW Induction Motor (°C)

	f (Hz)			
T (%)	**12.5**	**25**	**37.5**	**50**
125	63	61	63	69
115	63	61	63	69
100	**63**	**63**	**63**	**69**
75	63	62	63	69
50	63	62	62	69
25	63	61	62	69

Appendix 2

The analyzed miscellaneous output calculated by analyzing model:

Table I. Analyzed power factors computed via analyzing model

	f (Hz)			
T (%)	**12.5**	**25**	**37.5**	**50**
125	0.8573	0.8215	0.8075	0.8055
115	0.8449	0.8022	0.7903	0.7891
100	**0.8182**	**0.7724**	**0.7527**	**0.7660**
75	0.7271	0.6716	0.6656	0.6830
50	0.5579	0.5357	0.5085	0.5240
25	0.2855	0.2623	0.2297	0.3094

Table II. Analyzed stator impedance computed via analyzing model

	f (Hz)			
T (%)	**12.5**	**25**	**37.5**	**50**
125	0.5895+0.4492i	0.5895+0.8983i	0.5895+1.3475i	0.5895+1.7966i
115	0.5895+0.4492i	0.5895+0.8983i	0.5895+1.3475i	0.5895+1.7966i
100	**0.5895+0.4492i**	**0.5895+0.8983i**	**0.5895+1.3475i**	**0.5895+1.7966i**
75	0.5895+0.4492i	0.5895+0.8983i	0.5895+1.3475i	0.5895+1.7966i
50	0.5895+0.4492i	0.5895+0.8983i	0.5895+1.3475i	0.5895+1.7966i
25	0.5895+0.4492i	0.5895+0.8983i	0.5895+1.3475i	0.5895+1.7966i

Table III. Analyzed rotor impedance computed via analyzing model

	f (Hz)			
T (%)	**12.5**	**25**	**37.5**	**50**
125	4.0493+0.4539i	9.3899+0.9077i	14.8668+1.3616i	19.6701+1.8154i
115	4.5330+0.4539i	10.7064+0.9077i	16.6016+1.3616i	21.9072+1.8154i
100	**5.4450+0.4539i**	**12.5798+0.9077i**	**20.1065+1.3616i**	**24.8403+1.8155i**
75	8.2517+0.4539i	18.7413+0.9077i	28.1454+1.3616i	35.0413+1.8155i
50	14.3529+0.4539i	28.8169+0.9077i	46.2904+1.3616i	58.5694+1.8155i
25	39.8909+0.4539i	80.2497+0.9077i	141.56+1.3616i	125.26+1.8155

Table IV. Analyzed maximum torque appeared via computing in the analyzing model

	f (Hz)			
T (%)	**12.5**	**25**	**37.5**	**50**
125	72.10	96.18	106.42	111.97
115	72.11	96.18	106.43	111.97
100	**72.11**	**96.18**	**106.43**	**111.97**
75	72.11	96.19	106.44	111.98
50	72.11	96.20	106.45	112.00
25	72.12	96.23	106.50	112.05

Appendix 3

M-file analyzing model below:

```
%%P00
close all
clear all
clc

% Rotor speed ********************************************************* Input
Q=1491;
% Experimental nominal torque (Nm)*********************************** Input
T_Exp=8.02;
% input frequency (Hz) ************************************************ Input
f=50;
%Line-to-line voltage star connected(V)****************************** Input
U=400;
Omega=2*pi*f; %Stator angular frequency (rad/s)
p=2; %Number of pole pairs
P=(T_Exp*Omega)/p;% Nominal power (W)
%Temperature rise in the stator windings (K)************************** Input
Theta=69;
%Temperature rise in the rotor windings (K)************************** Input
Theta2=Theta+10;
P01
P02
P03
P04
P05
P06
P07
P08
P09
P10
P11
P12
P13
P14
P15
P16
P17
P18
P19
P20
P21
P22
P23
P24
P25
P26
P27
P28
P29

%%P01
%% 1. Initial data
U_sph=U/((3)^(0.5)); %Phase voltage (V)
m=3; %Number of phases
```

```
n_syn=(60*f)/p; % Synchronous speed (1/min)
PF=0.9515; %Rated power factor, estimated
Eff=0.9; %Rated efficiency, initial estimated
Mu_0=4*pi*10^(-7); %Permeability of vacuum (VsA(-1)m(^-1))
Sigma_Cu20C=57*10^6; %Conductivity of copper at 20 degrees C (S/m)
Alfa_Cu=3.81*10^(-3); %Temperature coefficient of copper
Rho_Cu=8960; %Density of copper (kg/m3)
Sigma_Al20C=35.7*10^6; %Conductivity of aluminium at 20 degrees C (S/m)
Alfa_Al= 3.57*10^(-3); %Temperature coefficient of aluminium
Rho_Al=2700; %Density of aluminium (kg/m3)
k_Fe=0.97; %Space factor of stator and rotor core
Rho_Fe=7600; %Density of iron (kg/m3)
B=[0 0.1 0.2 0.3 0.4 0.5 0.6 0.7 0.8 0.9 1 1.1 1.2 1.3 1.4 1.5 1.6 1.7 1.8
1.9 2 2.1];
H=[0 84.5 107 121 133 145 156 168 180 194 209 228 254 304 402 660 1480 3710
7300 15000 30000 100000];
K_sat=[0 0.05 0.1 0.16 0.25 0.37 0.5 0.67 0.875 1.2 1.7];
a_i=[2/pi 0.66 0.68 0.7 0.72 0.74 0.76 0.78 0.8 0.82 0.84];
B_y=[0 0.1 0.2 0.3 0.4 0.5 0.6 0.7 0.8 0.9 1 1.1 1.2 1.3 1.4 1.5 1.6 1.7
1.8 1.9];
c= [0.72 0.72 0.72 0.72 0.72 0.72 0.71 0.7 0.67 0.63 0.57 0.48 0.4 0.33
0.26 0.2 0.17 0.16 0.15 0.14];
%The specific iron loss per mass at 1.5 T and 50 Hz with M800-65 A
P_15=6.74; % (W/kg)
 figure(1)
 plot (H,B) %BH curve of M800-50
 xlabel('H')
 ylabel('B')
 hold on
 figure(2)
 plot (K_sat, a_i) %
 xlabel('K_sat')
 ylabel('a_i')
 hold on
 figure(3)
 plot(B_y,c)
 xlabel('B_y')
 ylabel('c')
 hold on

%%P02
%% 2. Tangential stress
Sigma_Ftan=15000*(PF/0.8);
%The determination of the main dimensions starts with choosing the
appropriate
% tangential stress according to the machine type  (Table 6.3)

%%P03
%% 3. Rotor size
n_n=Q; % (min -1)
T=P/(2*pi*((n_n)/60)); %The rated torque estimate (Nm)
V_r=T/(2*Sigma_Ftan); %The volume Vr (m3)
%The ratio of equivalent core length and air-gap diameter is according to
Table 6.5
X=((pi)*(p^(1/3)))/(2*p);
D_r=((4*V_r)/(pi*X))^(1/3); %From the equations above we can solve the
rotor diameter and the equivalent iron core length(m)
D_r=0.124;
```

```
l_rounded=X*D_r; %We select a rounded number (m)
l_rounded=0.16+0.001; % (m)

%%P04
%% 4. Air gap and core length
%The air-gap length is, depending on the number of pole pairs, calculated
%from Eqs. (6.41) and (6.42)
%In this case, p = 2 and the air gap is calculated from
Delta=(0.18+0.006*(P)^(0.4))/1000;
% or
Delta_new=Delta*1.6; %In heavy-duty applications, the air gap is increased
by 60 %. We use in this case an increased air gap
Delta_new= 0.0005; %(m)We select a rounded number for the air gap
D_s=D_r+2*Delta_new; %The inner diameter of the stator [m]
n_V=0; b_v=0; b_ve=0; %As there are no cooling channels
l=l_rounded-2*Delta_new; %Core length in a machine with no cooling channels

%%P05
%% 5. Stator and rotor windings
q=4; %The number of stator slots per pole and phase q is chosen
W_winding_pitch=5/6; %the winding pitch
Q_s=2*p*m*q; %The number of stator slots
Tau_us=pi*(D_s/Q_s); %The stator slot pitch (m)
Tau_p=pi*(D_s/(2*p)); %The stator pole pitch (m)
 %We select a skewed rotor. According to Tables 7.3 and 7.5,
Q_r=40;
Tau_ur=pi*(D_r/Q_r); %The rotor slot pitch tur will be (mm)

%%P06
%% 6. Air-gap flux density and linear current density
%Since the tangential stress has already been selected, the amplitude of
%the fundamental of the air-gap flux density has to correlate with the
%selected stress value, which was the average value. According to Table 6.1
%the peak value of the fundamental air-gap flux density varies normally
from
%0.7 T to 0.9 T. Let us choose for the fundamental air-gap flux peak
density
B_1peak=0.8; % (T)
%0.7 T to 0.9 T. Let us choose for the fundamental air-gap flux peak
density
A=(((2^(0.5))*Sigma_Ftan)/(B_1peak*PF)); % (A/m)
%We may solve for the RMS linear current density in Mathcad format

%%P07
%% 7. Number of coil turns in a phase winding
%The number of coil turns in series in a phase winding can be calculated
%according to Eq. (7.7) in the textbook
E_m=0.94*(U/(3^(0.5)));
%where Em is the air-gap-induced voltage that is here assumed to be
k_w1=((2*sin(W_winding_pitch*(pi/2)))*sin(pi/(m*2)))/(((Q_s*sin(pi*(p/Q_s))
)/(m*p)));%and kw1 the winding factor for the fundamental(Eq. (2.61)v = 1)
Alfa_li=0.67; %Initial value of the saturation factor ai
N_s=((E_m*(2)^(0.5))/(Omega*k_w1*Alfa_li*B_1peak*Tau_p*l_rounded));

%%P08
%% 8. Number of conductors in a slot
%The number of parallel branches
```

```
Alfa=2;
%The number of parallel branches
Z_Qs=2*Alfa*m*(N_s/Q_s);
Z_Qs=32; % we select
%the number of coil turns in the phase winding will be
N_s=((Q_s*Z_Qs)/(2*Alfa*m));

%%P09
%% 9.  New B1 peak
%The rounding of zQ influences the air-gap flux density. The saturation
%factor ai in Eq. (7.7) has to be iterated (We return from Item 13
%to this point). The original unsaturated value was ai = 2/p. We insert
%the value found in Item 13 (e.g. after the third iteration round)
Alfa_2i=0.693;
%The new air-gap flux density is [T]
B_1peak=((((2)^(0.5))*E_m)/(N_s*Omega*k_w1*Alfa_2i*Tau_p*l_rounded));

%%P10
%% 10. Width of the stator slot
%According to Table 6.1, the flux density of a stator tooth varies normally
%from 1.4 T to 2.1 T and the rotor tooth from 1.5 to 2.2 T.
%Let us choose for the apparent flux densities
B_dapps=1.6; % (T)
B_dappr=1.6; % (T)
%The apparent flux density according to the textbook is
%The tooth width is
b_ds=((((l_rounded*Tau_us)/(k_Fe*(l-(n_V*b_v)))))*(B_1peak/B_dapps)); % (m)
%The rotor tooth width is correspondingly
b_dr=(((l_rounded*Tau_ur)/(k_Fe*(l-(n_V*b_v))))*(B_1peak/B_dappr)); % (m)

%%P11
%% 11. Slot dimensions
%To determine the stator slot dimensions, we have first to estimate the
%stator current, Eq. (7.9a). The initial guess for the stator current is
I_s=P/(m*Eff*U_sph*PF);
J_s=3.5*10^6; %A/m^2
S_cs=I_s/(Alfa*J_s); % m^2
%kCu,s is the space factor of the slot. The space factor inside the slot
%insulation is about
K_Cus=0.63;
%With this value of the space factor, the wound area of the slot should be
at least
S_Cus=(Z_Qs*S_cs)/K_Cus; %[m^2]
%dimensions are presented below
b_1s=0.003; %m
h_1s=0.001; %m
h_2s=0.002; %m
h_3s=0.005; %m
h_6s=0.0005; %m
h_s=0.0005; %m
%Other dimensions are determined as follows
b_4s=(pi*(D_s+2*(h_1s+h_2s))/Q_s)-b_ds; %m
b_4cs=b_4s+((2*pi*h_3s)/Q_s)-(2*h_6s); %m
%The height h5 is determined so that the tooth width bd is constant and
%the wound area of the slot SCus has the value calculated above.
%The following two equations are used to solve h5
%The slot separator h_s is assumed zero. Its influence has been taken into
```

```
%account in the space factor kCus. The user must give an iteration value
for h5s to match SCus
h_5s=0.016; %[m]
b_5cs=b_4cs+((2*pi*h_5s)/Q_s);
S_Cus_New=(((b_4cs+b_5cs)/2)*h_5s)+ ((pi/8)*(b_5cs)^2);
%The value h5s given above satisfies the equations with sufficient
accuracy.
%b5s gets the value
b_5s=b_5cs+2*h_6s;
h_4s=h_5s+(b_5cs/2);
%The total area of the slot is needed later in the calculations
S_slot=b_1s*h_1s+h_2s*((b_4s/2)+(b_1s/2))+h_3s*(b_4s+((pi*h_3s)/(Q_s)))+(((
b_4s+b_5s)/2)*h_5s)+((pi/8)*(b_5s)^2); %[m^2]
%The rotor slot dimensions are calculated next
%The rotor current referred to the stator is approximately
I_r=I_s*PF;
%The transformation ratio between the rotor and stator currents is (Eq.
7.47)
K_rs1=(2*m*k_w1*N_s)/Q_r;
%The squirrel cage bar current is
I_bar=K_rs1*I_r;
%The rotor aluminium current density is selected according to Table 6.2
J_bar=3*10^6; %A/m^2 (Rotor winding) (3 .. 8) A/mm^2 for copper and (3..
6.5) A / mm2 for aluminium
J_ring=2.42*10^6; %A/m2 (short-circuit rings)
%As the die-cast-rotor slot space factor is kAlr = 1, the rotor slot area
%is equal to the bar cross-sectional area
S_bar=I_bar/J_bar; %m^2
S_Alr=S_bar; %m^2
%The rotor short-circuit ring current is calculated as (Eq. 7.38)
Alfa_uv=(2*pi)/Q_r; %rad
I_ring=I_bar/(2*sin(Alfa_uv/2)); % (A)
%The end ring cross-sectional surface is
S_ring=I_ring/J_ring;
%We can choose the following dimensions
b_1r=0.0007; % m
h_1r=0.002; %m
h_2r=0.003; %m
%Other dimensions are determined similarly as for the stator.
b_4r=(pi*(D_r-2*(h_1r+h_2r))/Q_r)-b_dr;
%The height h5r is determined so that the tooth width bdr remains constant
%and the wound area of the slot SAlr has the value calculated above. The
%following equations are used to solve h5r. We start with an initial guess
for h5r
h_5r=0.012; %m
b_5r=b_4r-((2*pi*h_5r)/Q_r);%m
h_4r=h_5r+(b_5r/2);
S_Alr=((b_4r+b_5r)/2)*h_5r+((pi/8)*b_5r^2)+(((b_1r+b_4r)*h_2r)/2);

%%P12
%% 12. Magnetic voltages over the stator and rotor teeth
%The flux density in the tooth is obtained by solving the intersection of
%the BH curve of the electric sheet in question and the line
%The flux density in the tooth is obtained by solving the intersection of
%the BH curve of the electric sheet in question and the line
%Initial guess
xx=linspace(B(1),B(end));
pp= spline(H,B);
```

```
v_s=ppval(pp, xx);

B_es=B_dapps;
B_er=B_dappr;

H_es = interp1(B,H,B_es);
H_er = interp1(B,H,B_er);

B_es=B_dapps-(((l_rounded*Tau_us)/(k_Fe*l*b_ds))-1)*Mu_0*H_es;

B_ds=B_es; %T
H_ds = interp1(B,H,B_ds);

B_er=B_dappr-(((l_rounded*Tau_us)/(k_Fe*l*b_dr))-1)*Mu_0*H_er;
B_dr=B_er; %T

H_dr = interp1(B,H,B_dr);

U_mds=H_ds*(h_3s+h_5s);
U_mdr=H_ds*(h_5r);

%%P13
%% 13. Magnetic voltage of the air gap and saturation factor
%The magnetic voltage of the air gap is calculated according to Eqs. (3.7b)
and (3.8)
NL=((1+(b_1s/(2*Delta_new))^2)^(0.5)); %%%%
k=(2/pi)*[atan(b_1s/(2*Delta_new))-((2*Delta_new)/(b_1s))*log(NL)];
k_C1s=Tau_us/(Tau_us-k*b_1s);
Delta_e=k_C1s*Delta_new;
NL2=((1+(b_1r/(2*Delta_e))^2)^(0.5)); %%%%!!!
k_r=(2/pi)*[atan(b_1r/(2*Delta_e))-((2*Delta_e)/(b_1r))*log(NL2)];
k_C1r=Tau_ur/(Tau_ur-k*b_1r);
%The equivalent air gap
Delta_e=k_C1s*k_C1r*Delta_new;
%The magnetic voltage of the air gap is according to Eq. (3.35)
U_m_Delta_e=(B_1peak*Delta_e)/Mu_0;
%According to Eq. (7.6), the saturaton factor is calculated as
K_sat1=(U_mds+U_mdr)/U_m_Delta_e;
%With Fig 7.2 we get
xx=linspace(K_sat(1),K_sat(end));
pp= spline(K_sat,a_i);
v_s=ppval(pp, xx);
a_i2 = interp1(K_sat,a_i,K_sat1);

%If this value differs from the value of a2i used in Item 9, we must
%return to Item 9 and give a2i the value of ai2 and repeat the iteration
%until a2i = ai2

%%P14
%% 14. Stator and rotor yokes
%The maximum flux densities of the stator and rotor yokes are selected
%according to Table 6.1.
B_ys=1.3;
B_yr=1.3;
%Where the air-gap flux
Phi_m=Alfa_2i*B_1peak*Tau_p*l_rounded; % Vs
```

```
h_ys=Phi_m/(2*k_Fe*(l-n_V*b_v)*B_ys); % m
h_ys=0.022; % m [adjustment]
h_yr=Phi_m/(2*k_Fe*(l-n_V*b_v)*B_yr); % m
h_yr=0.01904; % m [adjustment]
% Stator diameters
D_ys=D_s+2*(h_1s+h_2s+h_3s+h_4s+h_6s)+h_ys;
D_se=D_ys+h_ys;
%Where
Tau_ys=(pi*D_ys)/(2*p); % m
D_yr=(D_r-h_yr-2*(h_1r+h_2r+h_4r)); % m
Tau_yr=(pi*D_yr)/(2*p); % m
%From the BH curve of M800-50A, we get for the maximum field strengths in
%the stator and rotor yokes

xx=linspace(B(1),B(end));
pp= spline(H,B);
v_s=ppval(pp, xx);

H_ymaxs = interp1(B,H,B_ys);%A/m
H_ymaxr = interp1(B,H,B_yr);%A/m


xx=linspace(B_y(1),B_y(end));
pp= spline(B_y,c);
v_s=ppval(pp, xx);
c_s=interp1(B_y,c,B_ys);
c_r=interp1(B_y,c,B_yr);

%The stator and rotor magnetic voltages are calculated as
U_mys=c_s*H_ymaxs*Tau_ys;
U_myr=c_r*H_ymaxr*Tau_yr;

%%P15
%% 15. Total magnetic voltage and magnetizing current
%The magnetic voltages are above
%The total magnetic voltage is
U_mtot=U_m_Delta_e+U_mds+U_mdr+(U_mys/2)+U_myr/2;
%from which the effective value of magnetizing current can be calculated
I_m=(U_mtot*pi*p)/(3*N_s*k_w1*(2)^(0.5)); % A

%%P16
%% 16. Stator resistance
%The average length lav of a coil turn (Eq. (5.2))
l_av=2*l+2.04*W_winding_pitch*Tau_p; % m
%The conductivity of copper wire at 100 degrees C (the temperature rise is
%Q = 70 K)
Sigma_Cu=(Sigma_Cu20C)/(1+Theta*Alfa_Cu); % S/m
%The DC resistance of a phase winding - mitattu 0.5895
R_s=(N_s*l_av)/(Sigma_Cu*Alfa*S_cs); % Ohm
R_s=0.5895;  % Ohm

%%P17
%% 17. Rotor resistance referred to stator
%The conductivity of aluminium at 100 degrees C at rated load
Sigma_Al=Sigma_Al20C/(1+Theta2*Alfa_Al);
%The DC resistance of a rotor bar is according to Eq. (5.1)
R_bar=l/(S_Alr*Sigma_Al);
```

```
%We assume that the end ring has the same height as the rotor bar h4 + h2
%and is located at depth h1. The average end-ring diameter is
D_ring=D_r-2*(h_1r+(0.025/2)); % m
D_ring=0.097;% m [Adjustment]
l_ring=pi*(D_ring/Q_r);
% The cross-sectional area of the ring is
R_ring=l_ring/(S_ring*Sigma_Al); % ohm
R_r=R_bar+(R_ring/(2*(sin((pi*p)/Q_r))^2)); % ohm
% The skewing is carried out in the rotor so that it corresponds to one
%stator slot pitch (Fig. 4.16)
s_sq=pi*(D_s/Q_s);
k_sq=(sin((s_sq/Tau_p)*(pi/2))/((s_sq/Tau_p)*(pi/2)));
Rho_v=((4*m)/(Q_r))*((N_s*k_w1)/k_sq)^2;
R_r_transpose=Rho_v*R_r; % ohm

%%P18
%% 18. Magnetizing inductance and reactance
%The effective air gap
Delta_ef=((U_m_Delta_e+U_mds+U_mdr+(U_mys/2)+(U_myr/2))/U_m_Delta_e)*Delta_
e; % [m]
%Calculation of magnetizing inductance (Eq. 3.110)
L_m=(m/2)*(2/pi)*Mu_0*l_rounded*(1/(2*p))*(4/pi)*(Tau_p/Delta_ef)*(k_w1*N_s
)^2;% [H]
%The mangnetizing reactance is
X_m=L_m*Omega;

%%P19
%%  19. Air-gap leakage inductances and reactances
Alfa_us=((p*2*pi)/Q_s);
%The air-gap leakage is calculated in two parts for 600 harmonics
n=1;
a_Last=300;
k_Delta_1=0;
while n<=a_Last

k_Delta_1_Old=(((((sin((1+2.*n*m)*W_winding_pitch*(pi/2)))*(sin((1+2.*n*m)*
q*Alfa_us/2))/(q*sin((1+2.*n*m)*Alfa_us/2))))/((1+2.*n*m)*k_w1))^2)+k_Delta
_1;
    k_Delta_1=k_Delta_1_Old;
    n=n+1;
end

n=-1;
a_Last=-300;
k_Delta_12=0;
while n>=a_Last

k_Delta_12_Old=(((((sin((1+2.*n*m)*W_winding_pitch*(pi/2)))*(sin((1+2.*n*m)
*q*Alfa_us/2))/(q*sin((1+2.*n*m)*Alfa_us/2))))/((1+2.*n*m)*k_w1))^2)+k_Delt
a_12;
    k_Delta_12=k_Delta_12_Old;
    n=n-1;
end
%Thus, the air-gap leakage factor is
Sigma_Delta_s=k_Delta_1+k_Delta_12;
%In asynchronous machines with a cage winding, the cage damps harmonics,
%and consequently, the air-gap inductance becomes less significant.
%This can be estimated empirically by multiplying the inductance obtained
```

```
%from Eq. (4.16) with a damping factor, usually of the magnitude 0.8.
%Hence, the air-gap leakage inductance is
L_Delta_s=0.8*Sigma_Delta_s*L_m; %H
%And the stator air-gap leakage reactance
X_Delta_s=L_Delta_s*2*pi*f; %Ohm
%The rotor air-gap leakage is calculated with Eq. (4.21)
Sigma_Delta_r=((pi^2)/3)*(p/Q_r)^2;
L_Delta_r=Sigma_Delta_r*L_m; %H
%and the rotor air-gap leakage reactance referred to the stator
X_Delta_r=L_Delta_r*2*pi*f; %Ohm

%%P20
%% 20. Slot leakage inductances and reactances
%Eq. (4.51)
Epsilon=1-W_winding_pitch;
%Eq. (4.53)
K_1=1-(9/16)*Epsilon;
K_2=1-(3/4)*Epsilon;
%Eq. (4.49)
Lambda_us=K_1*((h_4s-
h_s)/(3*b_4s))+K_2*((h_3s/b_4s)+(h_1s/b_1s)+(h_2s/(b_4s-
b_1s))*log(b_4s/b_1s))+(h_s/(4*b_4s));
%Eq. (4.30)
L_us=((4*m)/Q_s)*Mu_0*l_rounded*N_s^2*Lambda_us;
X_us=2*pi*f*L_us; % Ohm
%According to (4.32) we get for the rotor slot leakage
Lambda_ur=(h_4r/(3*b_4r))+(h_1r/b_1r)+0.66;
L_ur=Mu_0*l_rounded*1^2*Lambda_ur;
X_ur=2*pi*f*L_ur; % Ohm

%P21
%% 21. Tooth tip leakage inductances and reactances
%Eq. (4.62)
Lambda_ds=K_2*((5*(Delta_new/b_1s))/(5+4*(Delta_new/b_1s)));
%Eq. (4.30)
L_sigma_ds=((4*m)/Q_s)*Mu_0*l_rounded*Lambda_ds*N_s^2;
X_sigma_ds=2*pi*f*L_sigma_ds;
Lambda_dr=K_2*((5*Delta_new/b_1r)/(5+4*(Delta_new/b_1r)));
L_sigma_dr=Mu_0*l_rounded*Lambda_dr;
X_sigma_dr=2*pi*f*L_sigma_dr;

%%P22
%% 22. End winding leakage inductances and reactances
%The average length lw of the stator end winding
l_ew=0.0615; %m
l_w=0.382; %m
W_ew=0.165; %m
%The permeance factors according to Table 4.1
Lambda_lew=0.5;
Lambda_W=0.2;
Lambda_ws=2*l_ew*Lambda_lew+W_ew*Lambda_W;
%The end winding leakage inductance (Eq. 4.64)
L_ws=((4*m)/(Q_s))*q*(N_s^2)*Mu_0*Lambda_ws; % H
X_ws=2*pi*f*L_ws; % ohm

%P23
%% 23. Skew leakage inductance
```

```
% The skew leakage inductance is found as (Eq. 4.81)
Sigma_sq=1-k_sq^2;
%(Eq. 4.80)
L_sq=Sigma_sq*L_m; %H

%%P24
%% 24. Inductances and reactances referred to the stator
% The stator leakage inductance (Eq. 4.7)
L_s_sigma=L_Delta_s+L_us+L_sigma_ds+L_ws+L_sq;
%and the leakage reactance
X_s_sigma=L_s_sigma*Omega; %Ohm
% The magnetizing inductance Lm was calculated in Item 18
%The rotor bar leakage inductance (see Items 20 and 21)
L_Delta_r_transpose=9.2732*10^-4; % H
L_bar=L_ur+L_sigma_dr;% H
%The rotor end winding leakage is (see Item 22)
L_ring=1.7751*10^(-8); %H
%The rotor total leakage inductance (Eq. 7.92)
L_r_sigma=L_bar+(L_ring/(2*(sin((pi*p)/Q_r))^2));
%The inductance may be referred to the stator by multiplying with Eq.
(7.53)
L_r_sigma_transpose=L_r_sigma*Rho_v+L_Delta_r_transpose; % H

%%P25
%% 25. Core and mechanical losses
%To calculate the core losses, we need the masses of different iron parts.
%The total volume of the stator is:
V_s=(pi/4)*((D_se^2)-(D_s^2))*l; % (m^3)
%The volume of the stator yoke
V_ys=pi*(((D_se/2)^2)-((((D_se)/2)-h_ys)^2))*l;
%The mass of the stator yoke
m_ys=V_ys*k_Fe*Rho_Fe;
%The total volume of the stator slots
V_slots=Q_s*S_slot*l; %(m^3)
%The volume of the teeth
V_ds=V_s-V_ys-V_slots;
%The total mass of the teeth
m_ds=V_ds*k_Fe*Rho_Fe;
%The stator teeth (only the height h_5s)
m_ds_loss=k_Fe*Rho_Fe*Q_s*b_ds*h_5s*l; % (kg)
%Iron loss correction coefficients (Table 3.2)
k_Fed=1.8;
k_Fey=1.5;
%The core loss in the stator yoke is
P_Feys=k_Fey*P_15*((B_ys/1.5)^2)*m_ys*((f/50)^(3/2));%(W)
%The core loss of the tooth area is calculated using the mass mdsloss
defined above
B_ds=1.5979; % (T)
P_Feds=k_Fed*P_15*(((B_ds/1.5)^2)*m_ds_loss)*(f/50)^(3/2); %(W)
%The total iron losses are
P_Fe=P_Feys+P_Feds;
%Because of the low rotor fundamental frequency, the rotor iron losses are
%taken into account in the additional losses.
%The mechanical losses consisting of windage and ventilator losses
%are calculated from an experimental equation (Eq. (9.19), Table 9.2)
v_r=(pi*(n_syn/60)*D_r); % m/s
k_p=15; %(Ws2/m4)
P_p=k_p*D_r*(l+0.6*Tau_p)*v_r^2;
```

```
%%P26
%% 26. Equivalent circuit parameters
%The imaginary unit is used in the impedance calculations
j=(-1)^(0.5);
%The rotational speeds used in the following calculations vary from zero
%to synchronous speed (from 0 min-1 to 1500 min-1)

x=1:(60*(f/p));
%This x is seen as a subscript in the following calculations
n_x=((60*f)/p)*(x/n_syn);
%slip
s_x=((60*f-n_x*p)/(60*f))+10^(-10);
%The rotor skin effect is evaluated assuming the rotor bar to be a
rectangle.
%The resistance factor is (Eqs. 5.24 and 5.26)
%We use the total conductor height in the calculation
h_c=h_2r+h_4r;
Zeta_x=h_c*(0.5*Omega.*s_x*Mu_0*Sigma_Al*1).^(0.5);
K_R_x=Zeta_x.*((sinh(2.*Zeta_x)+sin(2.*Zeta_x))./(cosh(2.*Zeta_x)-
cos(2.*Zeta_x)));
%Rotor slip frequency:
f_rx=s_x*f;
%The corresponding rotor leakage inductance skin effect factor is (Eqs.
(4.57) and (4.58))
K_L_x=(3./(2.*Zeta_x)).*((sinh(2.*Zeta_x)-
sin(2.*Zeta_x))./(cosh(2.*Zeta_x)-cos(2.*Zeta_x)));
%The skin effect factors for the whole range of slip are depicted in
%the graph below and used for the next calculations.
 figure(4)
 plot(s_x,K_R_x)
 hold on
 plot(s_x,K_L_x)
 xlabel('Motor Slip')
 ylabel('Skin effect factors')
 legend('K_R','K_L')
 hold on
%The rotor resistance referred to the stator is
R_transpose_r_x=Rho_v*(R_bar*K_R_x+(R_ring/(2*(sin((pi*p)/Q_r))^2)));
%and the rotor leakage inductance referred to the stator is
L_transpose_r_x=Rho_v*(L_bar*K_L_x+(L_ring/(2*(sin((pi*p)/Q_r))^2)));
X_transpose_r_x=L_transpose_r_x*Omega;
X_transpose_Sigma_r=X_transpose_r_x;
%Rotor circuit impedance:
Z_transpose_r_x=(R_transpose_r_x./s_x)+i*X_transpose_Sigma_r;
%Core loss resistance:
R_Fe=(3*E_m^2)./P_Fe;
%Magnetizing circuit impedance:
Z_m=(R_Fe*X_m*i)/(R_Fe+X_m*i);
%Stator circuit impedance:
Z_s=R_s+X_s_sigma*i;
%Total impedance of the equivalent circuit:
Z_x=Z_s+((Z_m.*Z_transpose_r_x)./(Z_m+Z_transpose_r_x));

%%P27
%% 27. Rated load, stator and rotor current
%The motor currents and the output power are calculated at all relevant
speeds nx
```

```
%Stator current phasor:
%The index, e.g. 1474 (the value must be given), corresponds to a speed
%in min-1. The sentence below returns the corresponding current absolute
value
I_s_x=U_sph./Z_x;
%Air gap voltage:
E_m_x=U_sph-I_s_x.*Z_s;
%Rotor current phasor:
I_transpose_r_x=I_s_x.*(Z_m./(Z_m+Z_transpose_r_x));
%No-load current:
I_0_x=I_s_x-I_transpose_r_x;
%Mechanical losses:
P_mech_x=P_p.*(n_x./n_n).^3;
%Output power:
P_x=(m*((abs(I_transpose_r_x)).^2).*((1-s_x)./s_x).*R_transpose_r_x)-
P_mech_x;

%%P28
%%  28. Losses, efficiency, power factor and torque
%Resistive losses of the stator
P_Cus_x=m.*((abs(I_s_x)).^2).*R_s; % W
%Resistive losses of the rotor
P_Cur_x=m.*((abs(I_transpose_r_x)).^2).*R_transpose_r_x; % W
%Power factor:
CosPhii=real(I_s_x)./abs(I_s_x); % W
%Additional losses:
a=0;
if (f<13)
    a=0.0048;
elseif  (f>=13 && f<=26)
    a=0.0091;
elseif (f>26 && f<=38)
    a=0.0133;
elseif (f>38)
    a=0.0229;
end
P_ad=a*(T_Exp^2); % W
%P_ad=3.*abs(I_s_x).*U.*CosPhii*0.5*10^(-2); % W
%Core losses:
P_Fe_x=m.*((abs(E_m_x)).^2)./R_Fe; % W
%Total losses:
P_loss_tot_x=P_Cus_x+P_Cur_x+P_ad+P_Fe_x; % W
%Efficiency:
Eff_x=P_x./(P_x+P_loss_tot_x);
%Torque:
T_x=(((m.*(abs(I_transpose_r_x)).^2).*(R_transpose_r_x.*(1./s_x)))-
P_mech_x)./(2*pi*(f/p));
%Maximum Torque
T_x_max=max(T_x);
%Starting current:
I_s_1=62.9257; %A
%Starting torque:
T_1=44.6308; %NM
figure(5)
 plot(n_x,T_x)
 xlabel('Rotational Speed [1/s]')
 ylabel('Torque [Nm]')
 hold on
```

```
 figure(6)
 plot(P_x,Eff_x)
 xlabel('Output Power [W]')
 ylabel('Efficiency')
 hold on
 figure(7)
 plot(n_x,abs(I_s_x))
 xlabel('Rotational Speed [1/s]')
 ylabel('Stator Current [A]')
 hold on
 figure(8)
 plot(P_x,CosPhii)
 xlabel('Output Power [W]')
 ylabel('Power Factor')
 hold on

%P29
%%
clc
disp('Stator current')%************************************coming from P27
disp(abs(I_s_x(Q)))

disp('Input power')
P_IN=P_loss_tot_x+P_x;
disp(abs(P_IN(Q)))

disp('Mechanical Torque')%*********************************coming from P28
disp(T_x(Q))

disp('P_Copper_stator')%************************************coming from P28
disp(P_Cus_x(Q))

disp('P_Copper_Rotor')%*************************************coming from P28
disp(P_Cur_x(Q))

disp('P_Iron calculated with first method')%*************coming from P25
disp(P_Fe)

disp('P_Iron calculated with second method')%************coming from P28
disp(P_Fe_x(Q))

disp('P_additional loss')%**********************************coming from P28
disp(P_ad)

disp('P_mechanical loss')%**********************************coming from P27
disp(P_mech_x(Q))

disp('Total losses')%***************************************coming from P28
disp(P_loss_tot_x(Q))

disp('Output power')%***************************************coming from P27
disp(P_x(Q))

disp('Efficiency')%*****************************************coming from P28
disp(Eff_x(Q))
```

```
disp('Power Factor')%************************************coming from P28
disp(CosPhii(Q))

disp('Stator impedance')%********************************coming from P26
disp(Z_s)

disp('Rotor impedance')%*********************************coming from P26
disp(Z_transpose_r_x(Q))

disp('Maximum Torque')%**********************************coming from P28
disp(T_x_max)
```